



Nonlinear Dynamic Stability Analysis of Axially Moving CNTRC Piezoelectric Viscoelastic Nano/Micro Plate Based on MCST

Pezhman Sourani ^a, Ali Ghorbanpour Arani ^{a,b,*}, Mohammad Hashemian ^c, Shahriar Niknejad ^a

^a Department of Solid Mechanics, Faculty of Mechanical Engineering, University of Kashan, Kashan, Iran

^b Institute of Nanoscience & Nanotechnology University of Kashan, Kashan, Iran

^c Department of Mechanical Engineering, Khomeinishahr Branch, Islamic Azad University, Khomeinishahr/Isfahan, Iran

Abstract

Analyzing the nonlinear dynamic stability of axially moving carbon nanotube reinforced composite (CNTRC) piezoelectric viscoelastic nano/micro plate under time dependent harmonic biaxial loading is the purpose of the present study. The nano/micro plate is made from Polyvinylidene Fluoride (PVDF). It moves in the positive direction of the x-axis at a constant velocity and supported by a nonlinear viscoelastic piezoelectric foundation (Zinc Oxide). A viscoelastic material is assumed in the Kelvin-Voigt model. Nano/micro plate is exposed to electric potential, 2D magnetic field and uniform thermal gradient. Maxwell's relations are used to integrate magnetic field effects. The nano/micro plate as well as smart foundation are subjected to electric potential in thickness direction. The effective elastic properties are estimated using the Eshelby-Mori-Tanaka approach. Von-Kármán's theory provides the basis for the nonlinear strain-displacement relationship. According to various shear deformation plate theories, a novel formulation is presented that incorporates surface stress effects via Gurtin-Murdoch elasticity theory. A modified couple stress theory (MCST) is used in order to consider small scale parameter. It is possible to derive the governing equations by using the energy method and Hamilton's principle. An analysis is conducted using Galerkin procedure and finally the incremental harmonic balance method (IHB) to obtain the dynamic instability region (DIR). Among the parameters that will be examined in this study are small-scale parameter, alternating and direct applied voltages, magnetic field intensity, surface effects as well as axially moving speed. The results demonstrate that increasing the axial speed of the nano/micro plate causes the system to become more unstable. As a result, if the smart foundation is considered, in addition to increasing the excitation frequency, the area of the instability zone will also decrease by at least 50%. It is estimated that in a static state (not moving), the area of the instability zone is reduced by more than 70%.

Keywords: nonlinear dynamic stability; piezoelectric; composite nano/micro plate

* Corresponding author. Tel.: +983155913434; fax: +983155913444
E-mail address: aghorban@kashanu.ac.ir, a_ghorbanpour@yahoo.com

1. Introduction

There are many reasons for the importance of nanotechnology because the properties of materials change as the particles become smaller. In other words, the physical properties of materials change with physical changes. For example, properties such as color, weight, mechanical resistance and even electrical conductivity of a material change. For this reason, nanomaterials and, as a result, nanotechnology, are of great interest. Some metals, which are usually conductive, can be semi-conductors on a nano scale or even act as insulators and vice versa. As mentioned in Feynman's theory, on the nanoscale, materials can be produced atom by atom with desired structure and shape. Of course, in this case, the ratio of surface to volume is very significant. Therefore, surface effects should be investigated in the study of nanomaterials. This is a very important feature that occurs in reactions on the surface of materials. Nanotechnology itself is a vast field of science that provides many opportunities for the development of science. It covers almost all sciences, from basic sciences to aerospace sciences and more. In fact, nanotechnology is a basic science that has led to the development of all sciences and is therefore of special importance [1, 2].

One of the most important issues in the field of continuous environment mechanics is the effects of its size and performance on the mechanical behavior of a system. These effects have a significant effect on the mechanical behavior of the material when the particle size becomes very small, and the classical theories of the mechanics of continuous environments are not able to consider it. This point is very clear and visible especially on the atomic scale, whose structure is not so big compared to the internal atomic characteristics of matter. In fact, size effects arise due to the interference of two internal characteristic length scales, such as the distance between particles, and the external characteristic length, such as crack length. The main difference between a classical continuous medium model and a non-classical model is that in classical continuous medium mechanics, it is assumed that the amount of stress at a point depends on the amount of strain at that point. While in the non-classical continuous medium mechanics model, it is assumed that the stress at one point is a function of the amount of strain at all points of the object. This model originates from Eringen's research. Eringen's theory includes information about the energy between atoms and the internal size scale is introduced as a material parameter in the structural equations and has a good agreement with the experimental results [3, 4]. In this research, a more conventional non-classical theory than the Eringen theory (modified Couple stress) is used. This theory includes high-order stress, which explains the special and unique mechanical behavior and characteristics of materials, especially on a very small scale.

Introducing dynamic stability to elastic systems was accomplished for the first time by Bolotin. The main focus of this study is the analysis of dynamic stability. As far as the amplitude of fluctuations with time is concerned, a dynamic system is stable when its solution to the governing differential equations maintains convergence under corresponding initial conditions. Furthermore, a theorem is stable when a small deviation in the assumptions leads to a small deviation in the result. Depending on the initial conditions, a dynamic system is said to be in Lyapunov stability if its solution does not diverge from equilibrium. Thus, a bounded input leads to a bounded output. Otherwise, the system becomes unstable. Dynamic stability is defined as the tendency of the system's response to equilibrium with time regardless of the initial conditions. In mathematics, this is called asymptotic stability. During dynamic stability analysis, when the system is subjected to time-dependent loading, the aim is to identify system parameters that would cause the system to lose stability if they were not controlled. Dynamic stability analysis involves excitation via equation coefficients. In other words, the analysis of dynamic stability is characterized by differential equations with time-dependent coefficients. If an object is subjected to a dynamic loading, its dynamic responses may not lead to severe vibrations under a certain condition, in which case it is called dynamic stability. A system may have static stability, but it may be disturbed in terms of dynamic stability. In order to establish dynamic stability, the system must also be statically stable. As said, in the discussion of dynamic stability analysis, the goal is to identify and control parameters of the system that lead to an excessive increase in the range of system vibrations. Usually, there is no suitable analytical answer for such problems, but by using some methods, without having a complete solution for the system, some of its features can be extracted. Among the most prominent equations with time-varying coefficients, we can mention Mathieu equation. The dynamic response of these system increases continuously with the passage of time and eventually leads to the instability of the system response. For this reason, it is very important to investigate and analyze the dynamic stability of these types of systems. Elastic systems under intermittent and time-varying axial loading, cam follower mechanism and pendulum with movable support are common examples of parametric excitation systems. Dynamic stability can be defined as the ability of a system to return to a steady state of operation after experiencing certain disturbances. In general, different systems or characteristics may affect the concept of dynamic stability. Dynamic stability refers to the power system's ability to maintain operational stability for a longer period of time following a small or large disturbance with the help of automatic regulation and control devices. Dynamic stability is the way the system reacts to a disturbance over time [5, 6].

A composite material is a material that has two phases, matrix and reinforcement. At least 5% of the reinforcing phase should be used. The background phase surrounds the reinforcing phase and tries to keep it in its relative place. On the other hand, the reinforcing phase will improve the performance and mechanical properties of the composite material. Controlling the properties according to the need can be considered as one of the most important advantages of composite materials. Composite nanomaterials are those composite materials that have one or more components with dimensions less than 100 nanometers. The first phase of the composite material has a crystalline structure and is considered as a base or background and can be considered to be made of polymer, metal or ceramic. The second phase also consists of nanoparticles or nanotubes as reinforcements and fillers in line with specific goals such as strength, resistance, suitable electrical properties, etc [7, 8].

Crystals have a special geometric order in terms of the dispersion and distance of components, which is often not the same in all directions. Unlike crystals, in amorphous or non-crystalline solids, the dispersion and distance of its components are the same in all directions. These non-crystalline solids are called isotropic or isotropic solids. Since most of the physical properties of crystalline solids are different in different directions, they are called anisotropic or non-isotropic. Only crystals that crystallize in a cubic device behave like non-crystalline bodies because they have the same dimensions in three spatial directions. The phenomenon of anisotropy creates properties in crystals that have different and important applications in industry. For example, if crystals such as quartz or polyvinylidene fluoride are pulled from both sides, in a direction perpendicular to the pressure or tension, they will have an electric charge in the opposite direction, and if we change the direction of this pressure or tension, the type of electric charge will also change. It changes that this phenomenon is called piezoelectric. Also, if an alternating electric current is connected to these crystals, the crystals expand and contract alternately and due to vibration, it leads to the production of sound. This feature is used as sound production, ultrasound, electric oscillations, crystal microphones and gramophone needles. Some crystals such as germanium, silicon and carbon have semi-conducting properties and conduct electric current to some extent. If semiconductor crystals are heated or exposed to light, their electrical resistance decreases and they pass electricity better. Piezoelectric polymers are considered smart materials. For this concept, other expressions such as active substances, adjustable or adaptable substances are also used. Smart materials refer to materials whose one or more properties are affected in response to an external operator. Currently, piezoelectric materials are widely used due to their fast electromechanical response and high power generation without the need for special tools. The production of electrical polarization in response to mechanical stress is an old Greek and common piezoelectric term for the pressure-electricity phenomenon. This event is known as direct effect [9, 10]. There are also piezoelectric materials with reverse effects, in which mechanical deformation is observed as soon as baroelectricity is applied to them. Due to the need for piezoelectric materials with high flexibility in special applications such as transducers and the lack of required ability in ceramics, polymers were researched and this feature was found in polyvinylidene fluoride (PVDF) compact form was discovered. This discovery was extremely important due to its very thin surfaces, high flexibility and piezoelectric properties. In recent years, piezoelectric polymer materials, especially polyvinylidene fluoride, have received the attention of scientific communities due to their superior characteristics, including excellent stability, resistance to wear, corrosion, and high strength, and many applications in devices They have nanoelectromechanics like nano sensors. On the other hand, CNTs can dramatically alter the properties of these materials. It is also more important than ever to investigate their dynamic stability and vibration. An intense vibration causes these structures to be unstable. The parametric resonance versus dynamic load factor is used for the description of dynamic instability region.

V. Bolotin [5] introduced dynamic stability to elastic systems for the first time. Many researchers continued to study dynamic stability after that. A. G. Arani et al. [11] discussed the vibration analysis of functionally graded nanocomposite plate moving in two directions. The results indicated that the natural frequency or stability of FG-CNTRC plate is strongly dependent on axially moving speed. K. Bouafia et al. [12] investigated the bending and free vibration characteristics of various compositions of FG plates on elastic foundation via quasi 3D HSDT model. They presented their results using a novel analytical model based on combined (cubic, sinusoidal and exponential) higher order formulation. M. Guellil et al. [13] analyzed the influences of porosity distributions and boundary conditions on mechanical bending response of FG plates resting on Pasternak foundation. R. S. Chahar, B. Kumar [14] studied the effectiveness of piezoelectric fiber reinforced composite (PFRC) laminate in active damping for smart structures. Using finite element method, the analysis reveals that the PFRC laminate can be used effectively for developing very light weight smart structures. N. Djilali et al. [15] evaluated the large cylindrical deflection analysis of FG carbon nanotube-reinforced plates in thermal environment using a simple integral HSDT. F. Abad et al. [16] discussed the application of the exact spectral element method in the analysis of the smart functionally graded plate. K. Draiche et al. [17] analyzed the computational flexural response of laminated composite plates using a simple quasi-3D HSDT. A. Ameri et al. [18] studied the hygro-thermo-mechanical bending of laminated composite plates

using an innovative computational four variable refined quasi-3D HSDT model. The analytical solution is derived via Navier's procedure. Q.-H. Pham et al. [19] investigated the static, free vibration and buckling response of functionally graded porous (FGP) nano plates resting on the Parternak's two-parameter elastic medium foundation. A. Attia et al. [20] discussed the free vibration of FG plates under thermal environment via a simple 4-unknown HSDT. Benchmark solutions are considered to evaluate the accuracy of the proposed model. Z. Wang, Y. Chen [21] studied the multi-physical field effects on nonlinear static stability behavior of nanoshell based on a numerical approach. More focus has been paid to the effects of small scale parameter, electric voltage and magnetic field intensity on stability curves of the nanoshell. M. A. Alazwari et al. [22] developed a nonclassical model to analyze bending response of microstructures considering surface stress under different loading and boundary conditions. F. Z. Kettaf et al. [23] presented the mechanical and thermal buckling analysis of laminated composite plates. F. Zhang et al. [24] studied the parametric vibration stability analysis of an axially moving plate with periodical distributed materials. It is investigated how the mass density and elastic modulus of the material affect the stability of the system. Floquet's theory is proven to be effective by numerical simulations. T. Cao, Y. Hu [25] presented magnetoelastic primary resonance and bifurcation of an axially moving ferromagnetic plate under harmonic magnetic field. A small variation of control parameters can have a dramatic effect on the system motion characteristics, as magnetic field strength, axial velocity, and mechanical load have significant effects on vibration characteristics. F. L. Yang et al. [26] accomplished the low-velocity impact response of axially moving functionally graded graphene platelet reinforced metal foam plates. graphene platelet reinforced metal foam (GPLRMF) plates moving axially exhibit significant impact response depending on foam distributions, different GPL patterns, GPL weight fractions, foam coefficients, plate speeds, impactor masses, and impact velocity. A. G. Arani et al. [27] described the instability analysis of axially moving sandwich plates with a magnetorheological elastomer core and GNP-reinforced face sheets. They used FSDT plate theory and Halpin-Tsai model to present their issue. In this paper, the effect of several parameters on the instability of the plate (critical speed) is examined, including the magnetic field intensity, the thickness of the MR core, the dispersion pattern, and the mass fraction of GNPs. Y. Wang et al. [28] studied the vibration and stability analysis of rectangular plates axially moving in fluid. Using classical plate theory, they found that with increasing fluid density or immersion level, the natural frequency of the submerged moving plates decreased. Y.-F. Zhou, Z.-M. Wang [29] analyzed the dynamic instability of axially moving viscoelastic plate. In order to analyze their results, they considered the Kelvin-Voigt model. A. G. Arani, T. Soleymani [30] implemented the size-dependent vibration analysis of an axially moving sandwich beam with MR core and axially FGM faces layers in yawed supersonic airflow. They presented their results based on modified first strain gradient theory (MMSGT) and Hamilton's principle. P. Hung et al. [31] investigated the Small scale thermal analysis of piezoelectric-piezomagnetic FG microplates using modified strain gradient theory. M. Arefi et al. [32] discussed the thermo-mechanical buckling behavior of FG GNP reinforced micro plate based on MSGT. Various theories and methods are used to verify the outputs of this work. A. Ghorbanpour Arani et al. [33] studied the pull-in instability of MSGT piezoelectric polymeric FG-SWCNTs reinforced nanocomposite considering surface stress effect. P. Kumar, S. Harsha [34] investigated the static, buckling and vibration response of three-layered functionally graded piezoelectric plate under thermo-electric mechanical environment. Virtual displacements and Von-Kármán displacement fields are used to obtain the governing equations of motion in first-order shear deformation theory (FSDT). A. Singh et al. [35] analyzed the viscoelastic free vibration analysis of in-plane functionally graded orthotropic plates integrated with piezoelectric sensors. Layer-wise functionally graded orthotropic plates are considered in this work using 3D elastic and viscoelastic free vibration formulations. Y. Zhao et al. [36] studied the nonlinear forced vibration of thermo-electro-elastic piezoelectric-graphene composite nanoplate based on viscoelastic foundation. Piezoelectric-graphene composite nanoresonators will undergo experimental characterization of their mechanical properties based on the dynamic results of this study. A. Sofiyev [37] discussed the dynamic stability of functionally graded viscoelastic plates with different initial conditions. Using the Galerkin method, the integro-differential equation system is solved. Z. Li et al. [38] presented the wave propagation analysis of porous functionally graded piezoelectric nanoplates with a visco-Pasternak foundation. Based on the Kelvin-Voigt model, the results demonstrate that the nonlocal parameters (NLPs) and length scale parameters (LSPs) have exactly the opposite effect on the frequency of the waves. P. H. Cong, N. D. Duc [39] analyzed the effect of nonlocal parameters and Kerr foundation on nonlinear static and dynamic stability of micro/nano plate with graphene platelet reinforcement. Airy stress functions, Galerkin method, and Runge-Kutta fourth-order method were used. M. H. Jalaei, H.-T [40] presented the dynamic stability analysis of viscoelastic porous FG nanoplate under longitudinal magnetic field via a nonlocal strain gradient quasi-3D theory. Navier and Bolotin's methods are used to calculate the unstable region. Q.-H. Pham, P.-C. Nguyen [41] investigated the dynamic stability analysis of porous functionally graded microplates using a refined isogeometric approach and MCST. J. Shi, X. Teng [42] studied the modified size-dependent dynamic stability and critical voltage of piezoelectric curved system. As a result of MCST and nonlocal theory, it was found that elastic foundation coefficients (Winkler and

Pasternak type), boundary conditions, voltage applied, size-dependent parameters (length scales and nonlocal ones), and geometry affect critical voltages and dynamic stability. Q. Li et al. [43] discussed the nonlinear dynamic stability analysis of axial impact loaded structures via the nonlocal strain gradient theory. This paper considers four types of axial impact loading configurations, namely sinusoidal, exponential, rectangular, and damping. Y. Zhang et al. [44] researched the nonlinear dynamic responses of functionally graded graphene platelet reinforced composite cantilever rotating warping plate. A. A. Daikh et al. [45] investigated the Static and dynamic stability responses of multilayer functionally graded carbon nanotubes reinforced composite nanoplates via quasi 3D nonlocal strain gradient theory. S. Lu et al. [46] studied the dynamic stability of axially moving graphene reinforced laminated composite plate under constant and varied velocities. X. Guo et al. [47] investigated the dynamic responses of a piezoelectric cantilever plate under high–low excitations. They found that high-low coupled resonant frequencies change the motion of the piezoelectric cantilever plate from stable to unstable. R. Abdikarimov et al. [48] studied the dynamic stability of orthotropic viscoelastic rectangular plate of an arbitrarily varying thickness. Results obtained from the viscoelastic problem with the exponential relaxation kernel almost match those obtained from the elastic problem. A. Shariati et al. [49] discussed the nonlinear dynamics and vibration of reinforced piezoelectric scale-dependent plates as a class of nonlinear Mathieu–Hill systems: parametric excitation analysis. According to the results, bifurcation point variation is determined by damping coefficient, while amplitude response is controlled by natural frequency term. J.-X. Wang et al. [50] investigated a novel composite joint with corrugated web and cover plates for simultaneously improving anti-collapse resistance and seismic behavior. Those configuration details have a significantly positive effect on the development of internal force, especially in the catenary mechanism stage to provide tensile force. C. Chu et al. [51] discussed the energy harvesting and dynamic response of shape memory alloys (SMA) nano conical panels with nanocomposite piezoelectric patch under moving load. using the FSDT and mixture rule, boron nitride nanotubes (BNNTs) with smart properties are used to reinforce the piezoelectric patch. They found that, increasing the weight fraction of Boron Nitride Nanotubes (BNNT) up to 0.4% in the piezoelectric layer was found to be a suitable strategy to simultaneously decrease the dimensionless dynamic displacement and enhance dimensionless voltage by 23.4% and 21%, respectively. P. Wan et al. [52] studied the application of Differential Quadrature Hierarchical Finite Element Method (DQHFEM) for free and forced vibration, energy absorption, and post-buckling analysis of a hybrid nanocomposite viscoelastic rhombic plate assuming CNTs' waviness and agglomeration. The structure is located on a viscoelastic torsional fractional substrate. Their results showed that, the weight percent of the CNTs affects the number of oscillations and changes the vibration pattern so that with increasing the CNTs content, the number of oscillations is enhanced.

In the author's knowledge, no report exists regarding the nonlinear biaxial dynamic stability analysis of SWCNTs reinforced piezoelectric viscoelastic nano/micro composite plate using Eshelby-Mori-Tanaka method based on MCST considering surface stress effects using various shear deformation plate theories and especially IHBM to determine DIR. In this article, the Galerkin method is applied to separate the parameters of time and space. Another innovation of this research is nonlinear viscoelastic piezoelectric foundation. The derivation of differential equations governing the problem according to various conditions such as electrical, mechanical, thermal and magnetic loading and also axially moving of nano/micro plate can be considered as the main and most important innovation of this research.

2. Fundamental formulation

2.1. Displacement field

The displacement field for nano/micro composite plate is as follows [53]:

$$u(x, y, z, t) = u_0(x, y, t) - zw_0(x, y, t)_{,x} + f(z) \left(w_0(x, y, t)_{,x} + \phi_x(x, y, t) \right), \quad (1)$$

$$v(x, y, z, t) = v_0(x, y, t) - zw_0(x, y, t)_{,y} + f(z) \left(w_0(x, y, t)_{,y} + \phi_y(x, y, t) \right), \quad (2)$$

$$w(x, y, z, t) = w_0(x, y, t). \quad (3)$$

where u, v, w describe an arbitrary point's displacement along x, y, z respectively. Furthermore, u_0, v_0, w_0 provide a representation of the corresponding displacements of the middle surface, and t is the time. According to the shape function $f(z)$, stress distributions and transverse shear deformations are described within nano/micro plate thickness. To determine the displacement field based on the shape function, there are various plate theories that can be used [53]:

(CPT, FSDT, RPT, SSDT, PSDPT, HSDPT, ESDPT):

$$f(z) = \left(0, z, z \left(1 - \frac{4z^2}{3h^2} \right), \left(\frac{h}{\pi} \sin \left(\frac{\pi z}{h} \right) \right), z \left(\frac{5}{4} - \frac{5z^2}{3h^2} \right), h \sinh \left(\frac{z}{h} \right) - z \cosh \left(\frac{1}{2} \right), ze^{-2(z/h)^2} \right) \tag{4}$$

2.2. Strain- displacement

According to Von-Kármán's theory, the nonlinear kinematic relations are as follows [53, 54]:

$$\epsilon_{xx} = u_{0,x} - zw_{0,xx} + f(z)(w_{0,xx} + \phi_{x,x}) + \frac{1}{2}w_{0,x}^2, \quad \epsilon_{yy} = v_{0,y} - zw_{0,yy} + f(z)(w_{0,yy} + \phi_{y,y}) + \frac{1}{2}w_{0,y}^2, \tag{5}$$

$$\gamma_{xy} = u_{0,y} + v_{0,x} + w_{0,x}w_{0,y} - 2zw_{0,xy} + f(z)(2w_{0,xy} + \phi_{x,y} + \phi_{y,x}), \tag{6}$$

$$\gamma_{xz} = f(z)_{,z}(w_{0,x} + \phi_x), \quad \gamma_{yz} = f(z)_{,z}(w_{0,y} + \phi_y). \tag{7}$$

2.3. Constitutive equations

The constitutive equations for the piezoelectric nano/micro composite plate are as follows [55]:

$$\begin{pmatrix} \sigma_{xx} \\ \sigma_{yy} \\ \sigma_{yz} \\ \sigma_{xz} \\ \sigma_{xy} \\ D_x \\ D_y \\ D_z \end{pmatrix} = \begin{pmatrix} Q_{11}\bar{g} & Q_{12}\bar{g} & 0 & 0 & 0 & 0 & 0 & -e_{31} \\ Q_{12}\bar{g} & Q_{22}\bar{g} & 0 & 0 & 0 & 0 & 0 & -e_{32} \\ 0 & 0 & Q_{44}\bar{g} & 0 & 0 & 0 & -e_{24} & 0 \\ 0 & 0 & 0 & Q_{55}\bar{g} & 0 & -e_{15} & 0 & 0 \\ 0 & 0 & 0 & 0 & Q_{66}\bar{g} & 0 & 0 & 0 \\ 0 & 0 & 0 & e_{15} & 0 & \zeta_{11} & 0 & 0 \\ 0 & 0 & e_{24} & 0 & 0 & 0 & \zeta_{22} & 0 \\ e_{31} & e_{32} & 0 & 0 & 0 & 0 & 0 & \zeta_{33} \end{pmatrix} \begin{pmatrix} (\epsilon_{xx} - \alpha_{xx}\Delta T) \\ (\epsilon_{yy} - \alpha_{yy}\Delta T) \\ \gamma_{yz} \\ \gamma_{xz} \\ \gamma_{xy} \\ E_x \\ E_y \\ E_z \end{pmatrix} + \begin{pmatrix} (Q_{13}/Q_{33})\sigma_{zz} \\ (Q_{23}/Q_{33})\sigma_{zz} \\ 0 \\ 0 \\ 0 \\ 0 \\ 0 \\ 0 \end{pmatrix}, \quad \bar{g} = 1 + g \frac{\partial}{\partial t}. \tag{8}$$

where g is structural damping constant based on Kelvin-Voigt model.

As previously stated, $\sigma_{ij}, D_i, \epsilon_{ij}, E_i$ are stress components, displacement by electricity, strain, and electric field respectively. $Q_{ij}, e_{ij}, \zeta_{ij}$ are also coefficients of stiffness matrix, piezoelectric and dielectric.

When the carbon nanofibers are angled within the matrix of a nano/micro composite plate [56]:

$$Q' = RQR^{-1}, \quad e' = ReR^{-1}, \quad \zeta' = R\zeta R^{-1} \tag{9}$$

$$R = \begin{bmatrix} n^2 & m^2 & 0 & 0 & -2nm \\ n^2 & m^2 & 0 & 0 & 2nm \\ 0 & 0 & n & m & 0 \\ 0 & 0 & -m & n & 0 \\ nm & nm & 0 & 0 & n^2 - m^2 \end{bmatrix}, \quad n = \cos(\alpha), \quad m = \sin(\alpha) \tag{10}$$

The following point should be noted that the component of stress σ_{zz} is ignored in comparison with other stress factors. This assumption, however, cannot be reconciled with a surface piezoelectricity theory. As a result, the assumption is that σ_{zz} satisfies both the upper and lower surface balance conditions, which can be calculated in the following manner [57]:

$$\sigma_{zz} = \left(\frac{1}{2} \quad \frac{z}{h} \right) \left(\left(\sigma_{xz,x}^s + \sigma_{yz,y}^s - \rho^s \ddot{w}_0 \right) \Big|_{S^+} + \left(\sigma_{xz,x}^s + \sigma_{yz,y}^s - \rho^s \ddot{w}_0 \right) \Big|_{S^-} \right) = \frac{2z}{h} \left(\tau^s w_{0,xx} + \tau^s w_{0,yy} - \rho^s \ddot{w}_0 \right). \quad (11)$$

2.4. Eshelby-Mori-Tanaka approach

CNT fibers are long and straight in this approach. Furthermore, the composite matrix presents a uniform distribution of fibers. The stiffness coefficients are stated as follows [55]:

$$\begin{pmatrix} \sigma_{xx} \\ \sigma_{yy} \\ \sigma_{zz} \\ \sigma_{yz} \\ \sigma_{xz} \\ \sigma_{xy} \end{pmatrix} = \begin{bmatrix} k+m & l & k-m & 0 & 0 & 0 \\ l & n & l & 0 & 0 & 0 \\ k-m & l & k+m & 0 & 0 & 0 \\ 0 & 0 & 0 & p & 0 & 0 \\ 0 & 0 & 0 & 0 & m & 0 \\ 0 & 0 & 0 & 0 & 0 & p \end{bmatrix} \begin{pmatrix} \varepsilon_{xx} \\ \varepsilon_{yy} \\ \varepsilon_{zz} \\ \gamma_{yz} \\ \gamma_{xz} \\ \gamma_{xy} \end{pmatrix}, \quad k, n, l, m, p \text{ are Hill's coefficients.} \quad (12)$$

so that k is the plane-strain bulk modulus normal to the fiber direction, n is the uniaxial tension modulus in the fiber direction, l is the associated cross modulus, m and p are the shear modulus in planes normal and parallel to the fiber direction, respectively. Based on the Mori–Tanaka method, the Hill's elastic moduli are obtained as follows [58]:

$$k = E_m \left\{ E_m c_m + 2k_r (1 + \nu_m) [1 + c_r (1 - 2\nu_m)] \right\} / 2(1 + \nu_m) [E_m (1 + c_r - 2\nu_m) + 2c_m k_r (1 - \nu_m - 2\nu_m^2)], \quad (13)$$

$$l = E_m \left\{ c_m \nu_m [E_m + 2k_r (1 + \nu_m)] + 2c_r l_r (1 - \nu_m^2) \right\} / (1 + \nu_m) [2c_m k_r (1 - \nu_m - 2\nu_m^2) + E_m (1 + c_r - 2\nu_m)], \quad (14)$$

$$n = E_m^2 c_m (1 + c_r - c_m \nu_m) + 2c_m c_r (k_r n_r - l_r^2) (1 + \nu_m)^2 (1 - 2\nu_m) / (1 + \nu_m) \left\{ 2c_m k_r (1 - \nu_m - 2\nu_m^2) + E_m (1 + c_r - 2\nu_m) \right\} + E_m [2c_m^2 k_r (1 - \nu_m) + c_r n_r (1 - 2\nu_m + c_r) - 4c_m l_r \nu_m] / 2c_m k_r (1 - \nu_m - 2\nu_m^2) + E_m (1 + c_r - 2\nu_m), \quad (15)$$

$$p = E_m [E_m c_m + 2(1 + c_r) p_r (1 + \nu_m)] / 2(1 + \nu_m) [E_m (1 + c_r) + 2c_m p_r (1 + \nu_m)], \quad (16)$$

$$m = E_m [E_m c_m + 2m_r (1 + \nu_m) (3 + c_r - 4\nu_m)] / 2(1 + \nu_m) \left\{ E_m [c_m + 4c_r (1 - \nu_m)] + 2c_m m_r (3 - \nu_m - 4\nu_m^2) \right\}. \quad (17)$$

3. Energy method

3.1. The strain energy

Based on MCST, strain energy can be expressed as follows [59]:

$$U = \frac{1}{2} \int_V (\sigma_{ij} \varepsilon_{ij} + m_{ij} \chi_{ij} - D_i E_i) dV, \quad (18)$$

$$\delta U = \int_V \left(\begin{array}{l} \sigma_{xx} \delta \varepsilon_{xx} + \sigma_{yy} \delta \varepsilon_{yy} + 2\sigma_{xy} \delta \varepsilon_{xy} + 2\sigma_{yz} \delta \varepsilon_{yz} + 2\sigma_{xz} \delta \varepsilon_{xz} \\ + m_{xx} \delta \chi_{xx} + m_{yy} \delta \chi_{yy} + m_{zz} \delta \chi_{zz} + 2m_{xy} \delta \chi_{xy} + 2m_{yz} \delta \chi_{yz} + 2m_{xz} \delta \chi_{xz} \\ - D_x \delta E_x - D_y \delta E_y - D_z \delta E_z \end{array} \right) dV, \quad (19)$$

The rotation vector θ , tensor of symmetric rotation gradient χ_{ij} are presented as follows:

$$m_{ij} = 2Gl^2 \chi_{ij}, \quad \chi_{ij} = \frac{1}{2} (\theta_{i,j} + \theta_{j,i}), \quad \theta_i = \frac{1}{2} e_{ijk} u_{k,j}, \quad G = \frac{E}{2(1+\nu)}. \quad (20)$$

$$\begin{pmatrix} \chi_{xx} \\ \chi_{yy} \\ \chi_{xy} \end{pmatrix} = \begin{pmatrix} w_{0,xy} - \frac{1}{2} f(z)_{,z} (w_{0,xy} + \phi_{y,x}) \\ -w_{0,xy} + \frac{1}{2} f(z)_{,z} (w_{0,xy} + \phi_{x,y}) \\ \frac{1}{2} (w_{0,yy} - w_{0,xx}) + \frac{1}{4} f(z)_{,z} (w_{0,xx} - w_{0,yy} + \phi_{x,x} - \phi_{y,y}) \end{pmatrix}, \quad (21)$$

$$\begin{pmatrix} \chi_{zz} \\ \chi_{xz} \\ \chi_{yz} \end{pmatrix} = \begin{pmatrix} \frac{1}{2} f(z)_{,z} (\phi_{y,x} - \phi_{x,y}) \\ \frac{1}{4} (v_{0,xx} - u_{0,yy}) + \frac{1}{4} f(z) (\phi_{y,xx} - \phi_{x,yy}) - \frac{1}{4} f(z)_{,zz} (w_{0,y} + \phi_y) \\ \frac{1}{4} (v_{0,xy} - u_{0,yy}) + \frac{1}{4} f(z) (\phi_{y,xy} - \phi_{x,yy}) + \frac{1}{4} f(z)_{,zz} (w_{0,x} + \phi_x) \end{pmatrix}. \tag{22}$$

3.2. The surface strain energy

In Gurtin and Murdoch's model, the thickness of the surface layer is assumed to be zero. As a result, the couple stress will not appear in the surface layer [57, 60].

The variation in surface strain energy of a nano/micro composite plate can be expressed as follows:

$$\delta U^s = \int_S (\sigma_{xx}^s \delta \epsilon_{xx} + \sigma_{yy}^s \delta \epsilon_{yy} + \sigma_{xz}^s \delta \gamma_{xz} + \sigma_{yz}^s \delta \gamma_{yz}) dS, \quad \begin{pmatrix} \sigma_{xx}^s \\ \sigma_{yy}^s \\ \sigma_{xz}^s \\ \sigma_{yz}^s \end{pmatrix} = \begin{pmatrix} (2\mu^s + \lambda^s) \epsilon_{xx} + \tau^s \\ (2\mu^s + \lambda^s) \epsilon_{yy} + \tau^s \\ \tau^s w_{0,x} \\ \tau^s w_{0,y} \end{pmatrix}, \tag{23}$$

μ^s, λ^s, τ^s refers to the Lamé surface constants and constant of residual stress, respectively.

3.3. The kinetic energy

The kinetic energy and surface kinetic energy of the nano/micro plate can be expressed as follows, [27, 29, 53, 56]:

$$\delta T = \int_{A-h/2}^{h/2} \rho \bar{V}^2 dz dA, \quad \delta T^s = \int_S \rho^s \bar{V}^2 dS, \tag{24}$$

$$\bar{V} = (C + \dot{u} + C u_{,x}) \bar{i} + (\dot{v} + C v_{,x}) \bar{j} + (\dot{w} + C w_{,x}) \bar{k}, \quad \frac{d}{dt} = \frac{\partial}{\partial t} + C \frac{\partial}{\partial x}. \tag{25}$$

\bar{V} is the absolute velocity vector and parameter C , represents the constant speed of the nano/micro plate.

3.4. External works

3.4.1. Nonlinear visco-piezoelectric foundation

Based on [33, 61, 62]:

$$\delta W_{foundation} = \iint (2V (e_{31f} w_{0,xx} + e_{32f} w_{0,yy}) + k_w w_0^3 + c_d \dot{w}_0) \delta w dz dA, \tag{26}$$

3.4.2. Electric field

An electric field can be expressed in terms of an electric potential. PVDF layer have the following electric potential distribution according to the Maxwell's equation:

$$E = -\nabla \varphi, \quad \varphi(x, y, z, t) = -\cos\left(\frac{\pi z}{h}\right) \varphi(x, y, t) + \frac{2z}{h} V e^{i\omega t}. \tag{27}$$

$$V = V_D + V_A \cos(\omega t), \quad V_D = \alpha_1 V_0, \quad V_A = \beta_1 V_0, \tag{28}$$

$$E_x = \cos\left(\frac{\pi z}{h}\right) \varphi_{,x}, \quad E_y = \cos\left(\frac{\pi z}{h}\right) \varphi_{,y}, \quad E_z = -\frac{\pi}{h} \sin\left(\frac{\pi z}{h}\right) \varphi - \frac{2}{h} V e^{i\omega t}. \tag{29}$$

In this equation, $\varphi(x, y, t)$ describes distribution of the time and spatial of the electric potential within the system. V_0 represents voltage from the external source of the system, and ω represents its natural frequency.

3.4.3. Magnetic field

It is possible to express the variations in external work caused by Lorentz force in the following manner. Maxwell's relations [63]. Due to the fact that 2D magnetic fields are applied in any direction in this study, the following relationships must be taken into account:

$$\vec{H} = (H_x, H_y, 0), \quad H_x = H \cos \theta, \quad H_y = H \sin \theta, \quad H^2 = H_x^2 + H_y^2, \quad (30)$$

where H is total applied magnetic field and θ is angle of between direction of 2D magnetic field and positive x-axis.

H_x, H_y are magnetic intensity in x and y direction, respectively.

$$\vec{h} = (H_y u_{,y} - H_x v_{,y} - H_x w_{,z}) \hat{i} + (-H_y w_{,z} - H_y u_{,x} + H_x v_{,x}) \hat{j} + (H_x w_{,x} + H_y w_{,y}) \hat{k}, \quad (31)$$

Considering Lorentz force in z direction [64]:

$$\bar{q}_{magnetic} = \int_{-h/2}^{h/2} f_z dz = \eta h (4H_x H_y w_{0,xy} + H_y^2 w_{0,yy} - H_y^2 w_{0,xx} - H_x^2 w_{0,yy} + H_x^2 w_{0,xx}). \quad (32)$$

where η describe the permeability of the magnetic field. Also \vec{h} is vectors of magnetic field disturbance.

3.5. Hamilton's principle

Hamilton's principle is used to derive the governing differential equations:

$$\int (\delta W_{ext} + (\delta U + \delta U^s) - (\delta T + \delta T^s)) dt = 0. \quad (33)$$

where $\delta W_{ext}, \delta U, \delta U^s, \delta T, \delta T^s$ assign each variable its corresponding work on external projects, energy generated by strain, energy associated with surface strain, kinetic energy, and surface kinetic energy variations.

4. Governing differential equations

The following motion equations can be obtained by combining Hamilton's principle with integration by parts and separating unknown coefficients:

$$\begin{aligned} \delta u_0 : N_{xx,x} + N_{xy,y} + \frac{1}{2}(X_{yz,yy} + X_{xz,xy}) + A_1(u_{0,xx} + w_{0,x} w_{0,xx}) - A_2 w_{0,xxx} + A_4(w_{0,xxx} + \phi_{x,xx}) = I_0(\ddot{u}_0 + 2C\dot{u}_{0,x} + C^2 u_{0,xx}) \\ - I_1(\ddot{w}_{0,x} + 2C\dot{w}_{0,x} + C^2 w_{0,xxx}) + I_3((\ddot{w}_{0,x} + \ddot{\phi}_x) + 2C(\dot{w}_{0,x} + \dot{\phi}_{x,x}) + C^2(w_{0,xxx} + \phi_{x,xx})), \end{aligned} \quad (34)$$

$$\begin{aligned} \delta v_0 : N_{xy,x} + N_{yy,y} - \frac{1}{2}(X_{yz,yy} + X_{xz,xy}) + A_1(v_{0,yy} + w_{0,y} w_{0,yy}) - A_2 w_{0,yyy} + A_4(w_{0,yyy} + \phi_{y,yy}) = I_0(\ddot{v}_0 + 2C\dot{v}_{0,y} + C^2 v_{0,yy}) \\ - I_1(\ddot{w}_{0,y} + 2C\dot{w}_{0,y} + C^2 w_{0,yyy}) + I_3((\ddot{w}_{0,y} + \ddot{\phi}_y) + 2C(\dot{w}_{0,y} + \dot{\phi}_{y,y}) + C^2(w_{0,yyy} + \phi_{y,yy})), \end{aligned} \quad (35)$$

$$\delta\phi_x : P_{xx,x} + P_{yy,y} - Q_{xz} + \frac{1}{2}(Y_{yy,y} - Y_{zz,z} + Y_{xy,x} + R_{yz,zy} + R_{xz,xy} - Z_{yz}) - A_4(u_{0,xx} - w_{0,x}w_{0,xx}) - A_5w_{0,xxx} + A_6(w_{0,xxx} + \phi_{x,xx}) + B_2w_{0,x} = I_3(\ddot{u}_0 + 2C\dot{u}_{0,x} + C^2u_{0,xx}) - I_4(\ddot{w}_{0,x} + 2C\dot{w}_{0,xx} + C^2w_{0,xxx}) + I_5((\ddot{w}_{0,x} + \ddot{\phi}_x) + 2C(\dot{w}_{0,xx} + \dot{\phi}_{x,x}) + C^2(w_{0,xxx} + \phi_{x,xx})), \tag{36}$$

$$\delta\phi_y : P_{xy,x} + P_{yy,y} - Q_{xz} - \frac{1}{2}(Y_{zz,z} - Y_{xx,x} + Y_{xy,y} + R_{yz,zy} + R_{xz,xy} - Z_{xz}) - A_4(v_{0,yy} - w_{0,y}w_{0,yy}) - A_5w_{0,yyy} + A_6(w_{0,yyy} + \phi_{y,yy}) + B_2w_{0,y} = I_3(\ddot{v}_0 + 2C\dot{v}_{0,y} + C^2v_{0,yy}) - I_4(\ddot{w}_{0,y} + 2C\dot{w}_{0,yy} + C^2w_{0,yyy}) + I_5((\ddot{w}_{0,y} + \ddot{\phi}_y) + 2C(\dot{w}_{0,yy} + \dot{\phi}_{y,y}) + C^2(w_{0,yyy} + \phi_{y,yy})), \tag{37}$$

$$\begin{aligned} \delta w_0 : & M_{xx,xx} + 2M_{xy,xy} + M_{yy,yy} + \bar{N} - X_{xx,xy} + X_{yy,xy} - X_{xy,yy} + X_{xy,xx} \\ & + A_1(u_{0,x}w_{0,xx} + v_{0,y}w_{0,yy} + \frac{1}{2}(w_{0,x}^2w_{0,xx} + w_{0,y}^2w_{0,yy})) + A_2(u_{0,xxx} + v_{0,yyy} + w_{0,x}w_{0,xxx} + w_{0,y}w_{0,yyy}) \\ & - A_3(w_{0,xxx} + w_{0,yyy}) + A_4((w_{0,xx} + \phi_{x,x})w_{0,xy} + (w_{0,y} + \phi_{y,y})w_{0,yy} - (w_{0,x}w_{0,xxx} + w_{0,y}^2w_{0,yy}) - (w_{0,y}w_{0,yyy} + w_{0,x}^2w_{0,yy}) - u_{0,xxx} - v_{0,yyy}) \\ & + A_5(2(w_{0,xxx} + w_{0,yyy}) + \phi_{x,xxx} + \phi_{y,yyy}) - A_6(w_{0,xxx} + \phi_{x,xxx} + w_{0,yyy} + \phi_{y,yyy}) + B_1(w_{0,xx} + w_{0,yy}) \\ & + B_2(w_{0,xx} + w_{0,yy}) - k_w w_0^3 - c_d \dot{w}_0 + \eta h(4H_x H_y w_{0,xy} + H_y^2 w_{0,yy} - H_x^2 w_{0,xx} - H_x^2 w_{0,yy} + H_x^2 w_{0,xx}) \\ & - 2(e_{31}w_{0,xx} + e_{32}w_{0,yy} + e_{31}^f w_{0,xx} + e_{32}^f w_{0,yy})V = I_0(\ddot{w}_0 + 2C\dot{w}_{0,x} + C^2w_{0,xx}) \\ & + (I_1 - I_3)(\ddot{u}_{0,x} + \ddot{v}_{0,y} + 2C(\dot{u}_{0,xx} + \dot{v}_{0,yy})) + C^2(u_{0,xxx} + v_{0,yyy}) - (I_2 - 2I_4 + I_5) \left(\begin{aligned} & \ddot{w}_{0,xx} + \ddot{w}_{0,yy} + 2C(\dot{w}_{0,xxx} + \dot{w}_{0,yyy}) \\ & + C^2(w_{0,xxxx} + w_{0,yyyy}) \end{aligned} \right) \\ & + (I_4 - I_5)(\ddot{\phi}_{x,x} + \ddot{\phi}_{y,y} + 2C(\dot{\phi}_{x,xx} + \dot{\phi}_{y,yy})) + C^2(\phi_{x,xxx} + \phi_{y,yyy}), \\ \delta\varphi : & \Psi_{x,x} + \Psi_{y,y} + \Psi_z = 0. \end{aligned} \tag{38}$$

$$\bar{N} = (N_{xx}w_{0,x} + N_{xy}w_{0,y})_{,x} + (N_{xy}w_{0,x} + N_{yy}w_{0,y})_{,y}, \tag{40}$$

$$\begin{pmatrix} I_0 \\ I_1 \\ I_2 \\ I_3 \\ I_4 \\ I_5 \end{pmatrix} = \left(\int_{-h/2}^{h/2} \rho \begin{pmatrix} 1 \\ z \\ z^2 \\ f(z) \\ zf(z) \\ f^2(z) \end{pmatrix} dz + \rho^s \begin{pmatrix} 1 \\ z \\ z^2 \\ f(z) \\ zf(z) \\ f^2(z) \end{pmatrix} \Big|_{z=\frac{h}{2}} + \rho^s \begin{pmatrix} 1 \\ z \\ z^2 \\ f(z) \\ zf(z) \\ f^2(z) \end{pmatrix} \Big|_{z=-\frac{h}{2}} \right), \tag{41}$$

$$\begin{pmatrix} A_1 \\ A_2 \\ A_3 \\ A_4 \\ A_5 \\ A_6 \end{pmatrix} = E^s \left(\begin{pmatrix} 1 \\ z \\ z^2 \\ f(z) \\ zf(z) \\ f^2(z) \end{pmatrix} \Big|_{z=\frac{h}{2}} + \begin{pmatrix} 1 \\ z \\ z^2 \\ f(z) \\ zf(z) \\ f^2(z) \end{pmatrix} \Big|_{z=-\frac{h}{2}} \right), \quad \begin{pmatrix} B_1 \\ B_2 \end{pmatrix} = \tau^s \left(\begin{pmatrix} 1 \\ (f(z),z) \end{pmatrix} \Big|_{z=\frac{h}{2}} + \begin{pmatrix} 1 \\ (f(z),z) \end{pmatrix} \Big|_{z=-\frac{h}{2}} \right). \tag{42}$$

$$N_{ii} = N_{ii}^M + N_{ii}^T + N_{ii}^E + N_{ii}^{sT} + N_{ii}^{sE}, \quad ii = xx, yy \tag{43}$$

$$N_{xx}^M, N_{yy}^M = N_{Static} + N_{Dynamic} \cos(\omega t), \quad N_{Static, Dynamic} = (\alpha, \beta)P^{or}, \tag{44}$$

$$N_{xx}^T = -h(Q_{11}\alpha_{xx} + Q_{12}\alpha_{yy})\Delta T, \quad N_{yy}^T = -h(Q_{12}\alpha_{xx} + Q_{22}\alpha_{yy})\Delta T, \tag{45}$$

$$N_{xx}^{sT} = -(Q_{11}^s\alpha_{xx}^s + Q_{12}^s\alpha_{yy}^s)\Delta T, \quad N_{yy}^{sT} = -(Q_{12}^s\alpha_{xx}^s + Q_{22}^s\alpha_{yy}^s)\Delta T, \tag{46}$$

$$N_{xx}^E = -e_{31}E_x h, \quad N_{yy}^E = -e_{32}E_y h, \quad N_{xx}^{sE} = -e_{31}^s E_x, \quad N_{yy}^{sE} = -e_{32}^s E_y, \quad N_{xy} = 0, \tag{47}$$

The stress resultants defined by:

$$(N_i, M_i, P_i) = \int_{-h/2}^{h/2} \sigma_i(1, z, f(z)) dz, \quad i = xx, yy, xy. \quad Q_i = k_s \int_{-h/2}^{h/2} \sigma_i f(z) dz, \quad i = yz, xz. \quad (48)$$

$$(X_i, Y_i) = \int_{-h/2}^{h/2} m_i(1, f(z)) dz, \quad i = xx, yy, zz, xy, yz, xz. \quad (49)$$

$$(R_i, Z_i) = \int_{-h/2}^{h/2} m_i(f(z), f(z)) dz, \quad i = yz, xz. \quad (50)$$

$$\Psi_i = \int_{-h/2}^{h/2} D_i \left(\cos \left(\frac{\pi z}{h} \right) \right) dz, \quad i = x, y, \quad \Psi_z = \int_{-h/2}^{h/2} D_z \left(\frac{\pi}{h} \sin \left(\frac{\pi z}{h} \right) \right) dz. \quad (51)$$

$$\begin{pmatrix} N_{xx} \\ N_{yy} \\ N_{xy} \\ M_{xx} \\ M_{yy} \\ M_{xy} \\ P_{xx} \\ P_{yy} \\ P_{xy} \end{pmatrix} = \begin{pmatrix} A_{11} & A_{12} & 0 & B_{11} & B_{12} & 0 & C_{11} & C_{12} & 0 \\ A_{12} & A_{11} & 0 & B_{12} & B_{11} & 0 & C_{12} & C_{11} & 0 \\ 0 & 0 & A_{66} & 0 & 0 & B_{66} & 0 & 0 & C_{66} \\ B_{11} & B_{12} & 0 & D_{11} & D_{12} & 0 & E_{11} & E_{12} & 0 \\ B_{12} & B_{11} & 0 & D_{12} & D_{11} & 0 & E_{12} & E_{11} & 0 \\ 0 & 0 & B_{66} & 0 & 0 & D_{66} & 0 & 0 & E_{66} \\ C_{11} & C_{12} & 0 & E_{11} & E_{12} & 0 & F_{11} & F_{12} & 0 \\ C_{12} & C_{11} & 0 & E_{12} & E_{11} & 0 & F_{12} & F_{11} & 0 \\ 0 & 0 & C_{66} & 0 & 0 & E_{66} & 0 & 0 & F_{66} \end{pmatrix} \begin{pmatrix} u_{0,x} + w_{0,x}^2 / 2 - \alpha_{xx} \Delta T \\ v_{0,y} + w_{0,y}^2 / 2 - \alpha_{yy} \Delta T \\ u_{0,y} + v_{0,x} + w_{0,x} w_{0,y} \\ -w_{0,xx} \\ -w_{0,yy} \\ -2w_{0,xy} \\ w_{0,xx} + \phi_{x,x} \\ w_{0,yy} + \phi_{y,y} \\ 2w_{0,xy} + \phi_{x,y} + \phi_{y,x} \end{pmatrix} - \begin{pmatrix} \bar{e}_1 \\ \bar{e}_2 \\ 0 \\ \bar{e}_3 \\ \bar{e}_4 \\ 0 \\ \bar{e}_5 \\ \bar{e}_6 \\ 0 \end{pmatrix}, \quad (52)$$

$$\begin{pmatrix} Q_{yz} \\ Q_{xz} \end{pmatrix} = \begin{pmatrix} A_{44} & 0 \\ 0 & A_{55} \end{pmatrix} \begin{pmatrix} w_{0,y} + \phi_y \\ w_{0,x} + \phi_x \end{pmatrix} - \begin{pmatrix} \bar{e}_7 \\ \bar{e}_8 \end{pmatrix}, \quad A_i = \int_{-h/2}^{h/2} Q_i(f(z)) dz, \quad i = 44, 55 \quad (53)$$

$$\begin{pmatrix} \bar{e}_1 \\ \bar{e}_2 \end{pmatrix} = - \begin{pmatrix} e_{31} \\ e_{32} \end{pmatrix} \left(P_{31} \frac{2}{h} V e^{i\alpha x} + A_{77} \varphi \right), \quad \begin{pmatrix} \bar{e}_3 \\ \bar{e}_4 \end{pmatrix} = - \begin{pmatrix} e_{31} \\ e_{32} \end{pmatrix} \left(P_{32} \frac{2}{h} V e^{i\alpha x} + B_{77} \varphi \right), \quad (54)$$

$$\begin{pmatrix} \bar{e}_5 \\ \bar{e}_6 \end{pmatrix} = - \begin{pmatrix} e_{31} \\ e_{32} \end{pmatrix} \left(P_{33} \frac{2}{h} V e^{i\alpha x} + C_{77} \varphi \right), \quad \begin{pmatrix} \bar{e}_7 \\ \bar{e}_8 \end{pmatrix} = D_{77} \begin{pmatrix} e_{24} \varphi_{,y} \\ e_{15} \varphi_{,x} \end{pmatrix}, \quad (55)$$

$$(A_i, B_i, C_i, D_i, E_i, F_i) = \int_{-h/2}^{h/2} Q_i(1, z, f(z), z^2, zf(z), f^2(z)) dz, \quad i = 11, 12, 66. \quad (56)$$

$$(A_{77}, B_{77}, C_{77}) = \int_{-h/2}^{h/2} \frac{\pi}{h} \sin \left(\frac{\pi z}{h} \right) (1, z, f(z)) dz, \quad D_{77} = \int_{-h/2}^{h/2} \cos \left(\frac{\pi z}{h} \right) f(z) dz, \quad (57)$$

4.1. Dimensionless groups

This procedure facilitates the continuation of the problem solving process as well as simplifying the governing equations and allowing comparison with other articles. Maple software is used to perform the dimensioning steps:

$$\begin{pmatrix} U, V, W \\ X, Y \\ \Theta_x, \Theta_y \\ \Psi \end{pmatrix} = \begin{pmatrix} (u_0, v_0, w_0) / h \\ x / a, y / b \\ \phi_x, \phi_y \\ \xi_{11} \varphi / e_{15} h \end{pmatrix}, \quad \tau = (t / h) \cdot (A_{11} / I_0)^{0.5}, \quad \begin{pmatrix} g^* \\ C^* \end{pmatrix} = \begin{pmatrix} g / t \\ C \cdot (A_{11} / I_0)^{-0.5} \end{pmatrix}, \quad (58)$$

5. Solving the governing differential equations

5.1. Galerkin method

This step involves discretizing dimensionless equations in space and time. By applying this technique, differential equations with partial derivatives are transformed into ordinary differential equations. After applying boundary conditions and multiplying the differential equations by appropriate coefficients (Acc. to table 1), the final differential equations are obtained. The Galerkin methodology includes considering the orthogonality condition of modes, which is one of the principles of this method, as well as double integration in length and width of the nano/micro plate. The harmonic solutions is considered in the following form [65]:

$$\begin{pmatrix} U(X,Y,\tau) \\ \Phi_x(X,Y,\tau) \end{pmatrix} = \begin{pmatrix} U'(\tau) \\ \Phi'_x(\tau) \end{pmatrix} \frac{\partial X_m(X)}{\partial X} Y_n(Y), \tag{59}$$

$$\begin{pmatrix} V(X,Y,\tau) \\ \Phi_y(X,Y,\tau) \end{pmatrix} = \begin{pmatrix} V'(\tau) \\ \Phi'_y(\tau) \end{pmatrix} X_m(X) \frac{\partial Y_n(Y)}{\partial Y}, \tag{60}$$

$$\begin{pmatrix} W(X,Y,\tau) \\ \Psi(X,Y,\tau) \end{pmatrix} = \begin{pmatrix} W'(\tau) \\ \Psi'(\tau) \end{pmatrix} X_m(X) Y_n(Y). \tag{61}$$

Table 1. The admissible functions for different boundary conditions

B.C.	X = 0	Y = 0	X = 1	Y = 1	X _m (X), (λ=mπ)	Y _n (Y), (μ=nπ)
SSSS	S	S	S	S	sin(λX),	sin(μY)
CSCS	C	S	C	S	sin ² (λX)	sin(μY)
CCCC	C	C	C	C	sin ² (λX)	sin ² (μY)
FCFC	F	C	F	C	cos ² (λX)[sin ² (λX)+1]	-

For simply supported boundary conditions:

$$\begin{pmatrix} U(X,Y,\tau) \\ \Phi_x(X,Y,\tau) \end{pmatrix} = \begin{pmatrix} U'(\tau) \\ \Phi'_x(\tau) \end{pmatrix} \cos(m\pi X) \sin(n\pi Y), \tag{62}$$

$$\begin{pmatrix} V(X,Y,\tau) \\ \Phi_y(X,Y,\tau) \end{pmatrix} = \begin{pmatrix} V'(\tau) \\ \Phi'_y(\tau) \end{pmatrix} \sin(m\pi X) \cos(n\pi Y), \tag{63}$$

$$\begin{pmatrix} W(X,Y,\tau) \\ \Psi(X,Y,\tau) \end{pmatrix} = \begin{pmatrix} W'(\tau) \\ \Psi'(\tau) \end{pmatrix} \sin(m\pi X) \sin(n\pi Y). \tag{64}$$

$$X = 0,1 \rightarrow V = W = N_{yy} = M_{xx} = \Phi_y = 0, \tag{65}$$

$$Y = 0,1 \rightarrow U = W = N_{xx} = M_{yy} = \Phi_x = 0. \tag{66}$$

$$\left(u_0 \quad or \quad M_{xx}^0 n_x + M_{xy}^0 n_y + \frac{1}{2} (\mu_{yz,y}^0 + \mu_{xz,x}^0) n_y \right) = 0, \tag{67}$$

$$\left(v_0 \quad or \quad M_{xy}^0 n_x + M_{yy}^0 n_y - \frac{1}{2} (\mu_{xz,x}^0 + \mu_{yz,y}^0) n_x \right) = 0, \tag{68}$$

$$\left(w_0 \quad or \quad \left(M_{xx}^0 w_{0,x} + M_{xy}^0 w_{0,y} + M_{xz}^0 + \frac{1}{2} (\mu_{xy,x}^0 + \mu_{yy,y}^0) \right) n_x \right. \\ \left. + \left(M_{xy}^0 w_{0,x} + M_{yy}^0 w_{0,y} + M_{yz}^0 - \frac{1}{2} (\mu_{xx,x}^0 + \mu_{xy,y}^0) \right) n_y \right) = 0, \tag{69}$$

$$M_{ij}^m = \int_{-h/2}^{h/2} \sigma_{ij} z^m dz, \quad \mu_{ij}^m = \int_{-h/2}^{h/2} m_{ij} z^m dz, \quad m = 0,1 \tag{70}$$

Electrical B.C.,

$$\int_V \begin{pmatrix} -D_x \\ -D_y \\ -D_z \end{pmatrix} \delta \begin{pmatrix} \cos\left(\frac{\pi z}{h}\right)\varphi_x \\ \cos\left(\frac{\pi z}{h}\right)\varphi_y \\ -\frac{\pi}{h}\sin\left(\frac{\pi z}{h}\right)\varphi - \frac{2}{h}Ve^{i\omega t} \end{pmatrix} dV = \begin{pmatrix} -\int_{\Gamma} \Psi_x \delta\varphi ds + \int_{\Omega_0} (\Psi_x)_{,x} \delta\varphi dx dy \\ -\int_{\Gamma} \Psi_y \delta\varphi ds + \int_{\Omega_0} (\Psi_y)_{,y} \delta\varphi dx dy \\ \int_{\Omega_0} \Psi_z \delta\varphi dx dy \end{pmatrix}. \tag{71}$$

$$\Psi_x n_x + \Psi_y n_y = 0. \tag{72}$$

Equations of motion in form of matrix:

$$[M]\ddot{Y} + [C^l + C^{nl}]\dot{Y} + [K^l + K^{nl}]Y = 0, \tag{73}$$

$$Y = \begin{pmatrix} U \\ V \\ \Theta_x \\ \Theta_y \\ W \\ \Psi \end{pmatrix}, \quad M = \begin{pmatrix} m_{11} & 0 & m_{13} & 0 & m_{15} & 0 \\ 0 & m_{22} & 0 & m_{24} & m_{25} & 0 \\ m_{31} & 0 & m_{33} & 0 & m_{35} & 0 \\ 0 & m_{42} & 0 & m_{44} & m_{45} & 0 \\ m_{51} & m_{52} & m_{53} & m_{54} & m_{55} & 0 \\ 0 & 0 & 0 & 0 & 0 & 0 \end{pmatrix}, \quad K_g = \begin{pmatrix} 0 & 0 & 0 & 0 & 0 & 0 \\ 0 & 0 & 0 & 0 & 0 & 0 \\ 0 & 0 & 0 & 0 & 0 & 0 \\ 0 & 0 & 0 & 0 & 0 & 0 \\ 0 & 0 & 0 & 0 & k_g & 0 \\ 0 & 0 & 0 & 0 & 0 & 0 \end{pmatrix}, \tag{74}$$

$$K^l = \begin{pmatrix} k_{11}^l & k_{12}^l & k_{13}^l & k_{14}^l & k_{15}^l & k_{16}^l \\ k_{21}^l & k_{22}^l & k_{23}^l & k_{24}^l & k_{25}^l & k_{26}^l \\ k_{31}^l & k_{32}^l & k_{33}^l & k_{34}^l & k_{35}^l & k_{36}^l \\ k_{41}^l & k_{42}^l & k_{43}^l & k_{44}^l & k_{45}^l & k_{46}^l \\ k_{51}^l & k_{52}^l & k_{53}^l & k_{54}^l & k_{55}^l & k_{56}^l \\ 0 & 0 & k_{63}^l & k_{64}^l & k_{65}^l & k_{66}^l \end{pmatrix}, \quad K^{nl} = \begin{pmatrix} 0 & 0 & 0 & 0 & k_{13}^{nl} & 0 \\ 0 & 0 & 0 & 0 & k_{23}^{nl} & 0 \\ 0 & 0 & 0 & 0 & k_{33}^{nl} & 0 \\ 0 & 0 & 0 & 0 & k_{43}^{nl} & 0 \\ 0 & 0 & 0 & 0 & k_{53}^{nl} & 0 \\ 0 & 0 & 0 & 0 & 0 & 0 \end{pmatrix}, \tag{75}$$

$$C^l = \begin{pmatrix} c_{11}^l & c_{12}^l & c_{13}^l & c_{14}^l & c_{15}^l & 0 \\ c_{21}^l & c_{22}^l & c_{23}^l & c_{24}^l & c_{25}^l & 0 \\ c_{31}^l & c_{32}^l & c_{33}^l & c_{34}^l & c_{35}^l & 0 \\ c_{41}^l & c_{42}^l & c_{43}^l & c_{44}^l & c_{45}^l & 0 \\ c_{51}^l & c_{52}^l & c_{53}^l & c_{54}^l & c_{55}^l & 0 \\ 0 & 0 & 0 & 0 & 0 & 0 \end{pmatrix}, \quad C^{nl} = \begin{pmatrix} 0 & 0 & 0 & 0 & c_{13}^{nl} & 0 \\ 0 & 0 & 0 & 0 & c_{23}^{nl} & 0 \\ 0 & 0 & 0 & 0 & c_{33}^{nl} & 0 \\ 0 & 0 & 0 & 0 & c_{43}^{nl} & 0 \\ 0 & 0 & 0 & 0 & c_{53}^{nl} & 0 \\ 0 & 0 & 0 & 0 & 0 & 0 \end{pmatrix}, \tag{76}$$

$$\begin{pmatrix} k_{13}^{nl} \\ k_{23}^{nl} \\ k_{33}^{nl} \\ k_{43}^{nl} \\ k_{53}^{nl} \\ k_{63}^{nl} \end{pmatrix} = \begin{pmatrix} 0 & 0 & 0 & 0 & \alpha_1 & 0 & \alpha_2 \\ 0 & 0 & 0 & 0 & \alpha_3 & 0 & \alpha_4 \\ 0 & 0 & 0 & 0 & \alpha_5 & 0 & \alpha_6 \\ 0 & 0 & 0 & 0 & \alpha_7 & 0 & \alpha_8 \\ \alpha_9 & \alpha_{10} & \alpha_{11} & \alpha_{12} & \alpha_{13} & \alpha_{14} & \alpha_{15} \\ 0 & 0 & 0 & 0 & 0 & 0 & 0 \end{pmatrix} \begin{pmatrix} U \\ V \\ \Phi_x \\ \Phi_y \\ W \\ W^2 \\ W_{,r} \end{pmatrix}, \quad \begin{pmatrix} c_{13}^{nl} \\ c_{23}^{nl} \\ c_{33}^{nl} \\ c_{43}^{nl} \\ c_{53}^{nl} \\ c_{63}^{nl} \end{pmatrix} = \begin{pmatrix} 0 & 0 & 0 & 0 & \alpha_2 & 0 & 0 \\ 0 & 0 & 0 & 0 & \alpha_4 & 0 & 0 \\ 0 & 0 & 0 & 0 & \alpha_6 & 0 & 0 \\ 0 & 0 & 0 & 0 & \alpha_8 & 0 & 0 \\ 0 & 0 & 0 & 0 & \alpha_{15} & 0 & 0 \\ 0 & 0 & 0 & 0 & 0 & 0 & 0 \end{pmatrix} \begin{pmatrix} U \\ V \\ \Phi_x \\ \Phi_y \\ W \\ W^2 \\ W_{,r} \end{pmatrix}. \tag{77}$$

where $Y, M, K^l, K^{nl}, C, C^{nl}$, representing a dimensionless displacement vector, mass matrix, linear stiffener matrix, nonlinear stiffener matrix, damping and nonlinear damping matrix, respectively. Appendix A and B provide the components of all matrices and their subset parameters.

5.2. Dynamic stability analysis

Harmonic load is applied to nano/micro plate [66]:

$$P(\tau) = (\alpha + \beta \cos(\Theta \tau)) P^{cr}, \quad \Theta = \hat{\Theta} h \sqrt{\frac{I_0}{A_{11}}}, \tag{78}$$

IHB method is an accurate method of analyzing dynamic stability. By substituting the harmonic solutions in the following equation [67]:

$$M\ddot{Y}(\tau) + C\dot{Y}(\tau) + \left[K_e - (\alpha + \beta \cos(\Theta \tau)) K_g \right] P^{cr} Y(\tau) = 0, \tag{79}$$

$$\omega^2 M \frac{d^2(Y(\bar{\tau}))}{d\bar{\tau}^2} + \omega C \frac{d(Y(\bar{\tau}))}{d\bar{\tau}} + (K^l + K^{nl} - (\alpha + \beta \cos(\hat{\tau})) K_g) Y(\bar{\tau}) = 0, \tag{80}$$

where, $\bar{\tau} = \Theta \tau$

$$Y(\bar{\tau}) = Y^*(\bar{\tau}) + \Delta Y(\bar{\tau}), \quad \beta = \beta^* + \Delta \beta, \quad \omega = \omega^* + \Delta \omega. \tag{81}$$

$$\omega^2 M \frac{d^2(\Delta Y(\bar{\tau}))}{d\bar{\tau}^2} + \omega^* C \frac{d(\Delta Y(\bar{\tau}))}{d\bar{\tau}} + (K^l + K^{nl} - (\alpha + \beta^* \cos(\bar{\tau})) K_g) \Delta Y(\bar{\tau}) = \tag{82}$$

$$R - \left(2\omega^* M \frac{d^2(Y^*(\bar{\tau}))}{d\bar{\tau}^2} + C \frac{d(Y^*(\bar{\tau}))}{d\bar{\tau}} \right) \Delta \omega + \cos(\bar{\tau}) K_g Y^*(\bar{\tau}) \Delta \beta,$$

$$R = - \left[\omega^{*2} M \frac{d^2(Y^*(\bar{\tau}))}{d\bar{\tau}^2} + \omega^* C \frac{d(Y^*(\bar{\tau}))}{d\bar{\tau}} + (K^l + K^{nl} - (\alpha + \beta^* \cos(\bar{\tau})) K_g) Y^*(\bar{\tau}) \right], \tag{83}$$

R is a correction term which is zero at boundary instability points.

$$Y_n^*(\bar{\tau}) = \sum_{i=1}^{N_h} \left\{ a_{n(2i-1)} \cos[(2i-1)\bar{\tau}] + b_{n(2i-1)} \sin[(2i-1)\bar{\tau}] \right\} = \eta_n A_n, \quad n = 1, 2, \dots, 6 \tag{84}$$

$$\Delta Y_n(\bar{\tau}) = \sum_{i=1}^{N_h} \left\{ \Delta a_{n(2i-1)} \cos[(2i-1)\bar{\tau}] + \Delta b_{n(2i-1)} \sin[(2i-1)\bar{\tau}] \right\} = \eta_n \Delta A_n, \tag{85}$$

where N_h is an integer selected according to the accuracy of the problem.

$$Y^*(\bar{\tau}) = \bar{Q} \cdot A, \quad \Delta Y(\bar{\tau}) = \bar{Q} \cdot \Delta A, \tag{86}$$

$$\bar{Q} = \begin{bmatrix} \eta & 0 & 0 & 0 \\ 0 & \eta & 0 & 0 \\ 0 & 0 & \ddots & 0 \\ 0 & 0 & 0 & \eta \end{bmatrix}_{n \times n}, \quad A = \begin{bmatrix} A_1 \\ A_2 \\ \vdots \\ A_n \end{bmatrix}, \quad \Delta A = \begin{bmatrix} \Delta A_1 \\ \Delta A_2 \\ \vdots \\ \Delta A_n \end{bmatrix}. \tag{87}$$

$$\int_0^{2\pi} \delta(\Delta Y(\bar{\tau}))^T \cdot \left[\omega^{*2} M \frac{d^2(\Delta Y(\bar{\tau}))}{d\bar{\tau}^2} + \omega^* C \frac{d(\Delta Y(\bar{\tau}))}{d\bar{\tau}} + (K^l + K^{nl} - (\alpha + \beta^* \cos(\bar{\tau})) K_g) \right] \Delta Y(\bar{\tau}) d\bar{\tau} \tag{88}$$

$$= \int_0^{2\pi} \delta(\Delta Y(\bar{\tau}))^T \cdot \left[R - \left(2\omega^* M \frac{d^2(Y^*(\bar{\tau}))}{d\bar{\tau}^2} + C \frac{d(Y^*(\bar{\tau}))}{d\bar{\tau}} \right) \Delta \omega + \cos(\bar{\tau}) K_g Y^*(\bar{\tau}) \Delta \beta \right] d\bar{\tau}.$$

$$S_1 \Delta A = R_1 + S_2 \Delta \omega + S_3 \Delta \beta, \tag{89}$$

$$S_1 = (\omega^*)^2 H_1 + \omega^* H_2 + H_3 + H_4 + H_5, \quad S_2 = -(2\omega^* H_1 + H_2) \cdot A, \quad S_3 = H_6 \cdot A, \tag{90}$$

$$R_1 = - \left((\omega^*)^2 H_1 + \omega^* H_2 + H_3 + H_4 + H_5 \right) \cdot A, \tag{91}$$

$$H_1 = \int_0^{2\pi} \bar{Q}^T M \bar{Q}_{,\bar{\tau}} d\bar{\tau}, \quad H_2 = \int_0^{2\pi} \bar{Q}^T C \bar{Q}_{,\bar{\tau}} d\bar{\tau}, \quad (92)$$

$$H_3 = \int_0^{2\pi} \bar{Q}^T K^l \bar{Q} d\bar{\tau}, \quad H_4 = \int_0^{2\pi} \bar{Q}^T K^{nl} \bar{Q} d\bar{\tau}, \quad (93)$$

$$H_5 = -\int_0^{2\pi} \bar{Q}^T (\alpha + \beta^* \cos(\bar{\tau})) K_g \bar{Q} d\bar{\tau}, \quad H_6 = -\int_0^{2\pi} \bar{Q}^T \cos(\bar{\tau}) K_g \bar{Q} d\bar{\tau}. \quad (94)$$

In this method, it is necessary to select one element of the vector A as a fixed reference with a zero increment. The first instability boundary is plotted in this analysis assuming $b_1 = 1, \Delta b_1 = 0$. On the other hand, the second instability boundary is represented by $b_2 = 1, \Delta b_2 = 0$. Additionally, the initial values of A, ω can be determined. furthermore, β is the known increment and is considered an independent variable. Calculation of $\Delta\omega, \Delta A$ is based on the initial values of the system of algebraic equations, and the secondary values of ω, A are based on $\omega + \Delta\omega, a_1 + \Delta a_1, b_1 + \Delta b_1$, continuing until the elements of the vector R are sufficiently small. $\Delta\beta$ is added to β and the process is repeated. The iterative process of this method is shown in Figure 1. $\varepsilon = 1e-9$

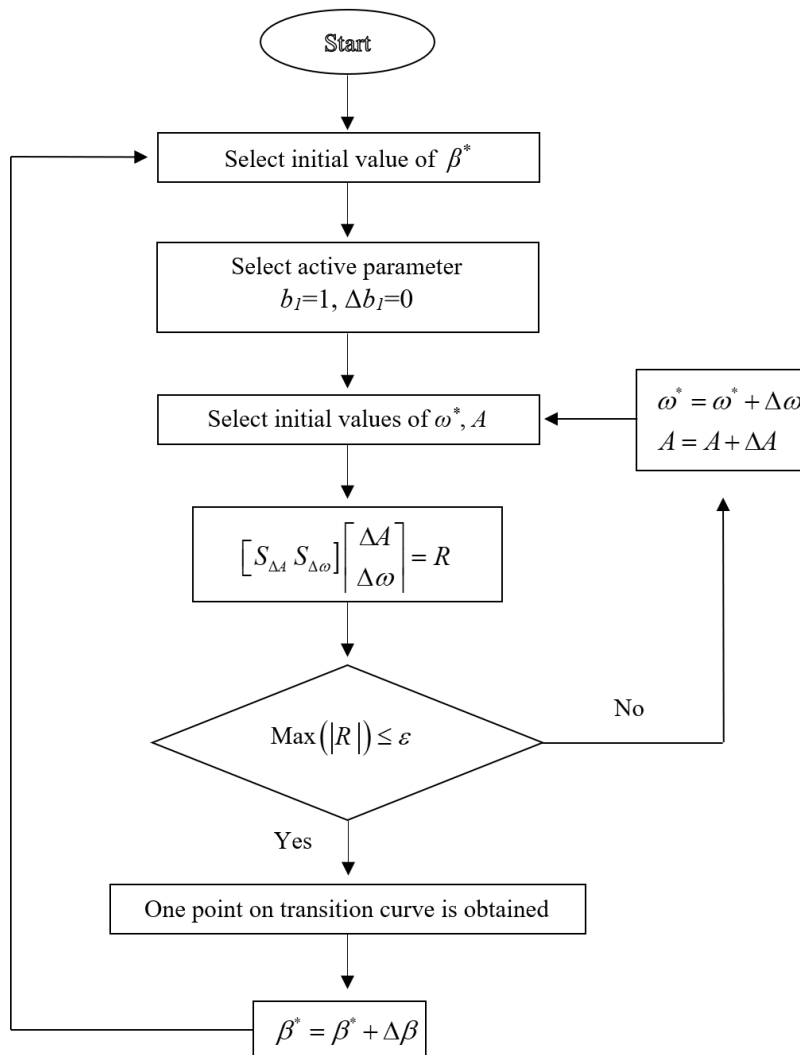


Fig 1: IHBM algorithm

6. Results and discussion

This part focuses on the impacts of small scale parameter, alternating and direct applied voltage, intensity of magnetic field, surface effects, thermal environment, static load factor and axially speed of nano/micro plate on the DIR. The viscoelastic piezoelectric nano/micro composite plate is made from PVDF and reinforced with SWCNTs. Table 2, lists their material properties [62]. Based on the authors' knowledge, there has not been a published study that examines the nonlinear dynamic stability of viscoelastic nano/micro plate under the conditions described in this paper. Since there are no references to such a work in the literature, it cannot be verified. Therefore, this paper is analyzed using a simplified method that does not consider surface effects, axially moving and several other factors. The findings of the present study are consistent with those of other studies. In table 3, the present work can be validated by comparing critical buckling load in various plate theories between the current article and the reference article [53]. In Fig. 3, the time response is illustrated for an arbitrary point within the region of dynamic instability. According to the graph, the response curve diverges in the region of instability, explaining the instability of the mentioned region and the validity of the study. Fig. 4, illustrates how the (l/h) parameter affects the dimensionless natural frequency. When the material length scale parameter approaches the thickness of the nano/micro plate, there is a significant difference in frequency between higher order and first order shear deformation plate theories. Fig. 5, presents the effect of axial speed of nano/micro plate on the DIR. As can be seen, if the smart foundation is considered, in addition to increasing the excitation frequency, the area of the instability zone will also decrease by at least 50%. In a static state, the nano/micro plate is estimated to reduce the area of instability by more than 70%. Based on MCST, fig. 6, shows the dynamic instability region of the piezoelectric nano/micro composite plate under direct and alternating voltages. The influence of direct voltages on parametric resonance is greater than that of alternating voltages. It should also be noted that a negative voltage has a greater impact on parametric resonance than other applied voltages. In the presence of a negative voltage, the piezoelectric nano/micro composite plate undergoes reverse polarization, becoming more stable as a result. Also, the dynamic instability region is larger for direct and alternating negative voltages as compared to other applied voltages. Fig. 7, illustrates how the piezoelectric polymeric nano/micro composite plate reinforced with SWCNTs responds to magnetic fields. Excitation frequencies increase with an increase in magnetic field. A piezoelectric nano/micro composite plate's excitation frequency is affected by its coefficient of residual surface stress in fig. 8. An increase in coefficient of residual stress is associated with an increase in nondimensional parametric resonance. The surface stress of nano/micro composite plate generates traction forces. As a result, the structure becomes more stable. As surface stress decreases, the dynamic stability region decreases. In this study, surface residual stress is considered positive. According to fig. 9,10 the primary nano/micro plate DIR is affected by low and high temperatures (thermal expansion coefficient with negative and positive values). It has been observed that different behaviors are displayed in these environments when the temperature is raised. A piezoelectric nano/micro composite plate is shown in fig. 11 to demonstrate how damping coefficient affect dynamic stability. As the damping coefficient of the system increase, the region of dynamic instability moves to lower excitation frequencies. Due to the increased energy damping produced by considering this parameter, the system is weaker and more susceptible to lower excitation frequencies. As shown in fig. 12, the static load factor affects the DIR for nano/micro plate. As the static loading factor increases, the initial DIR shifts to lower excitation frequencies. Additionally, it is reasonable to conclude that the nano/micro plate is more stable in the absence of static force. According to the equation related to the static load factor, increasing it reduces both the stiffness and frequency of the nano/micro plate. Fig. 13, shows the effect of the material length scale parameter on the dynamic instability region. As can be seen, the presence of the material length scale parameter tries to keep the system at higher excitation frequencies. Figures 14-17, demonstrate the frequency responses.

7. Conclusion

A generalized shape function is used to characterize transverse shear deformations for nonlinear dynamic stability analysis of viscoelastic piezoelectric nano/micro plate based on modified couple stress theory. The governing equations are derived based on Hamilton's principle. In order to validate the current formulation using IHB, numerical results obtained from the developed plate theory are compared with those reported in the literature. The present paper concludes that all higher order shear deformation plate theories considered in this paper provide similar results, and when the thickness of the nano/micro plate is comparable with the material length scale parameter, the difference between the Mindlin plate theory and higher order shear deformation plate theory is significant. Also, The following are some of the remarkable results:

- The smart foundation has a significant impact on the system stability control. This foundation reduces the area of dynamic instability region by more than 50% for a constant intensity of magnetic field.
- It was concluded that neglecting surface and small scale effects lead to inaccurate results in dynamic stability response of the system, since a remarkable difference obtained in cases of with and without surface effects.
- Due to the coefficients of surface stress increases, the parametric resonance increases.
- In contrast to alternating applied voltage, voltage applied directly has a greater influence on excitation frequencies.
- The modified couple stress theory predicts higher excitation frequencies than the classical theory.
- Dynamic instability region shifts to lower excitation frequencies as the damping coefficient of the structure increase.
- PSDPT,HSDPT,ESDPT have approximately the same results.
- The classical plate theory predicts a higher excitation frequency than other theories due to having a lower degree of freedom.

Table 2: Material properties

SWCNT	PVDF		ZnO
$E = 5.6466 \text{ TPa}$	$E = 8.3 \text{ GPa}$	$\nu = 0.18$	$e_{31} = -0.51 \text{ C/m}^2$
$G = 1.9445 \text{ TPa}$	$e_{31} = -0.130 \text{ C/m}^2$	$\rho = 1750 \text{ Kg/m}^3$	$e_{32} = -0.51 \text{ C/m}^2$
$\rho = 4000 \text{ Kg/m}^3$	$e_{32} = -0.450 \text{ C/m}^2$	$\epsilon_{11} = 1.1068 \text{ F/m}$	$e_{15} = -0.45 \text{ C/m}^2$
$\nu = 0.175$	$e_{15} = -0.009 \text{ C/m}^2$	$\epsilon_{22} = 1.1068 \text{ F/m}$	$e_{24} = -0.45 \text{ C/m}^2$
-	$e_{24} = -0.276 \text{ C/m}^2$	$\epsilon_{33} = 1.1068 \text{ F/m}$	-

Table 3: A comparison of critical buckling load

Theory	Present work ($l/h=0.8$)	Ref [53] ($l/h=0.8$)
CPT	33.2370	33.3892
FSDT	30.8814	30.9928
RPT	32.4033	32.6036
SSDT	33.5007	33.6102
PSDPT	32.5935	32.6036
HSDPT	32.5942	32.6038
ESDPT	32.6207	32.6310

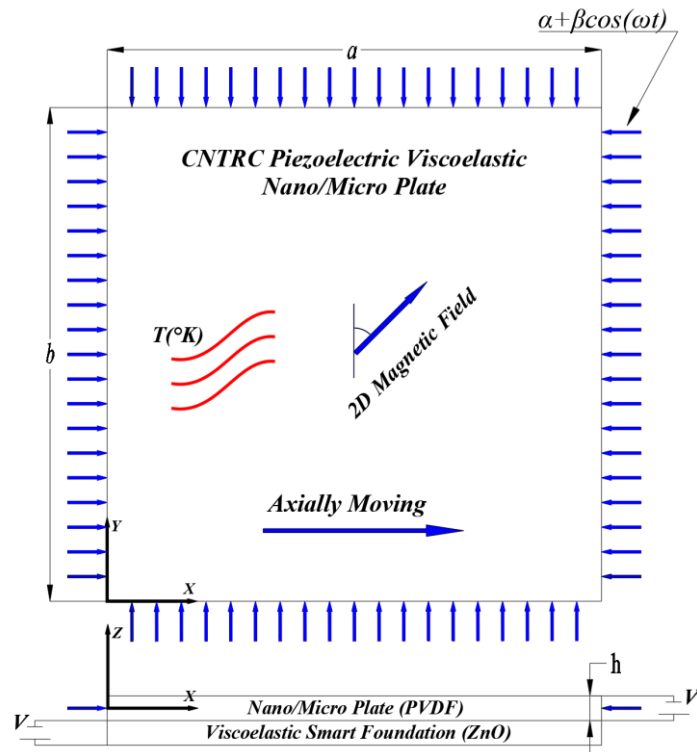


Fig 2: Graphical abstract

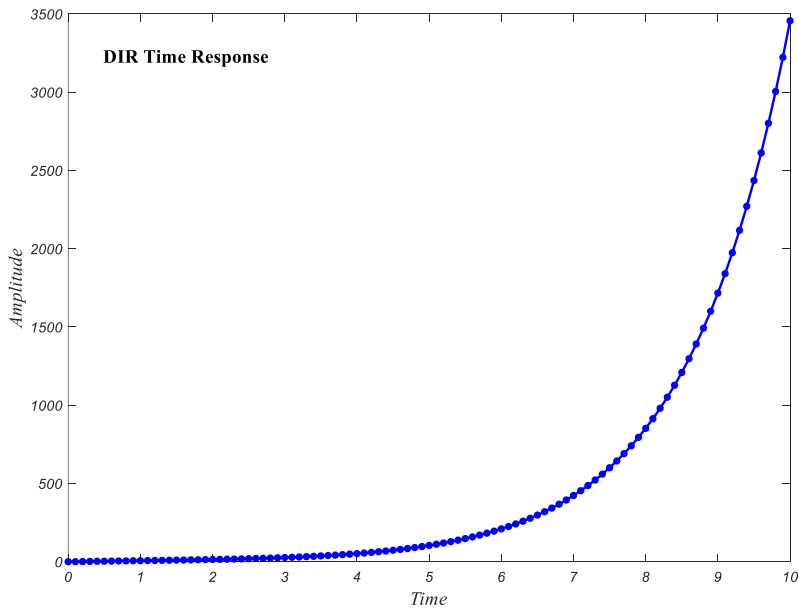


Fig 3: Time response of nano/micro plate for an arbitrary point within the DIR

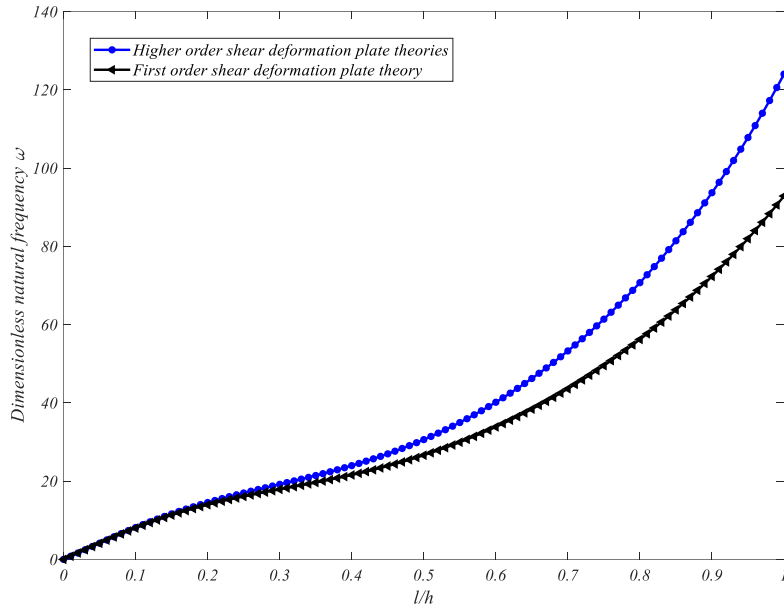


Fig 4: The effect of l/h parameter on the dimensionless natural frequency

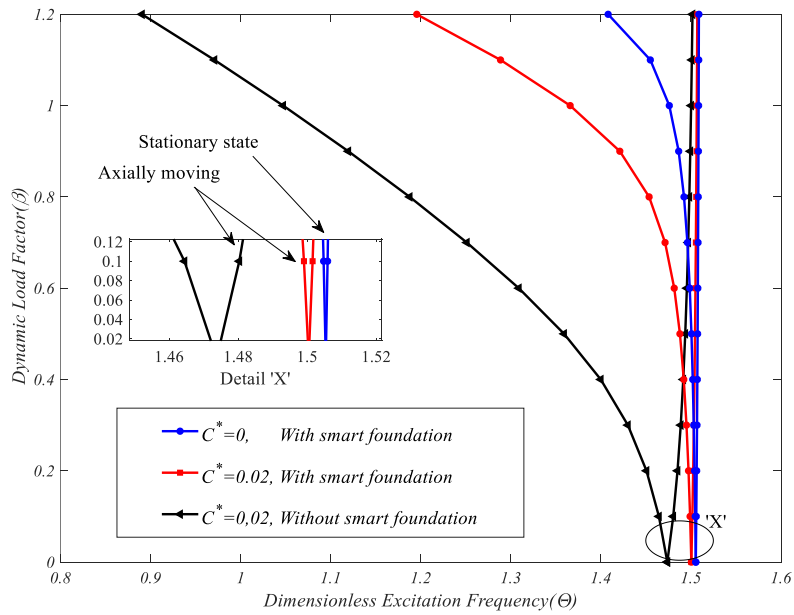


Fig 5: The effect of axial speed of nano/micro plate on the DIR

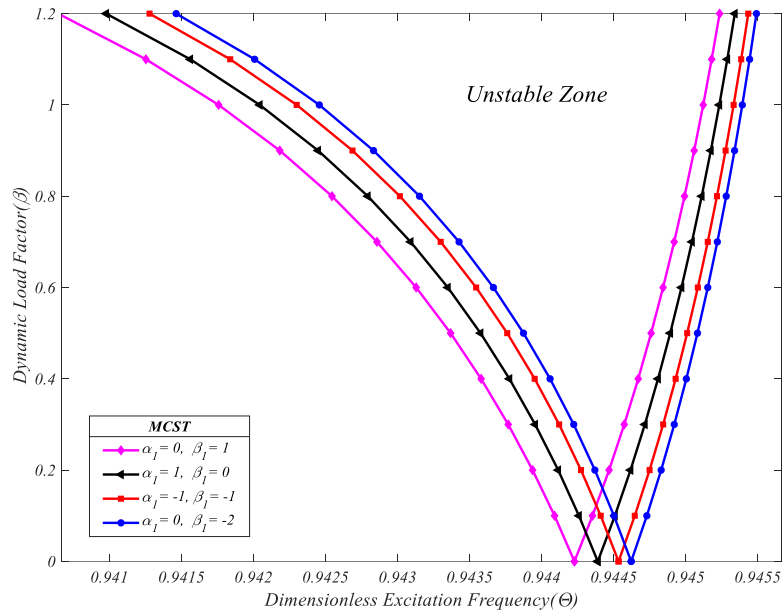


Fig 6: The effect of direct and alternating voltages on the DIR

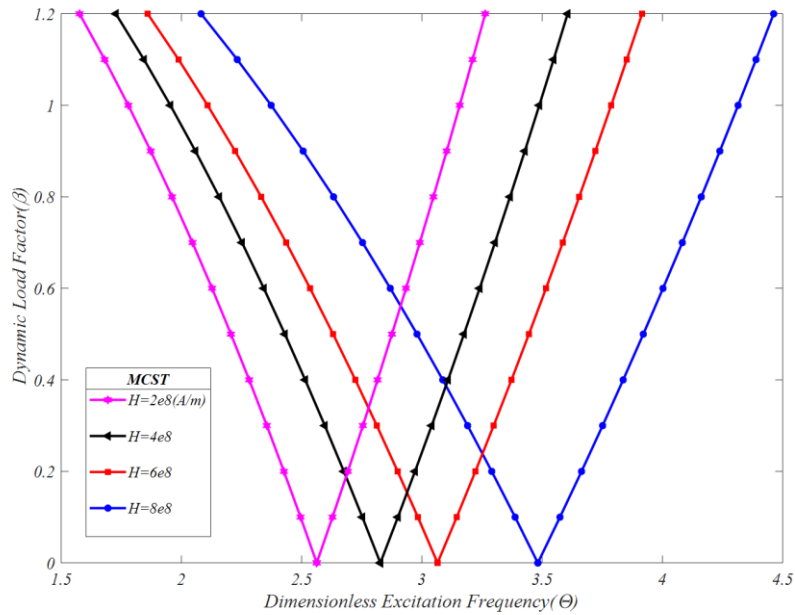


Fig 7: The effect of magnetic field on the DIR

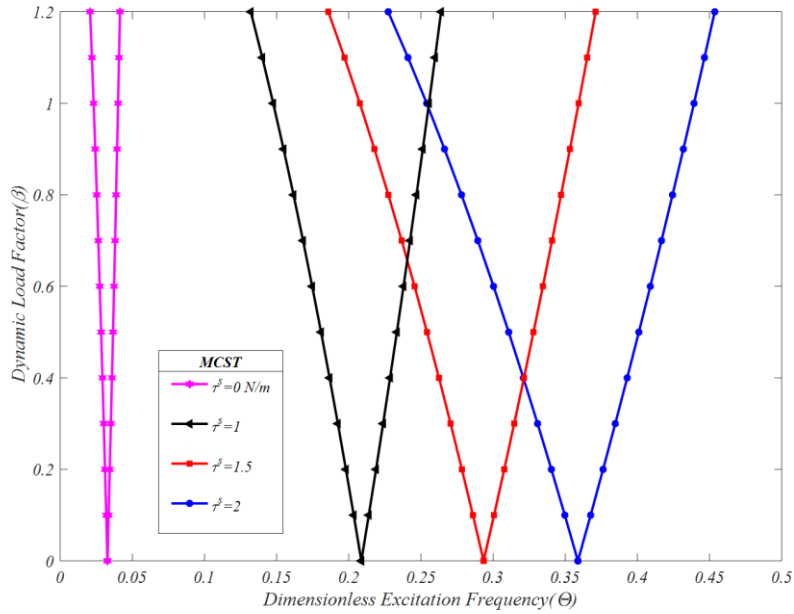


Fig 8: The effect of surface residual stress on the DIR

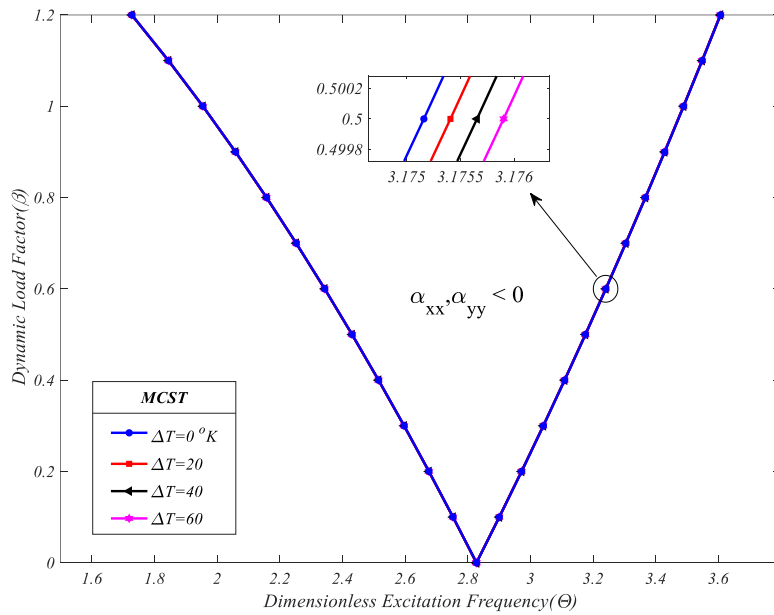


Fig 9: The effect of low temperature on the DIR

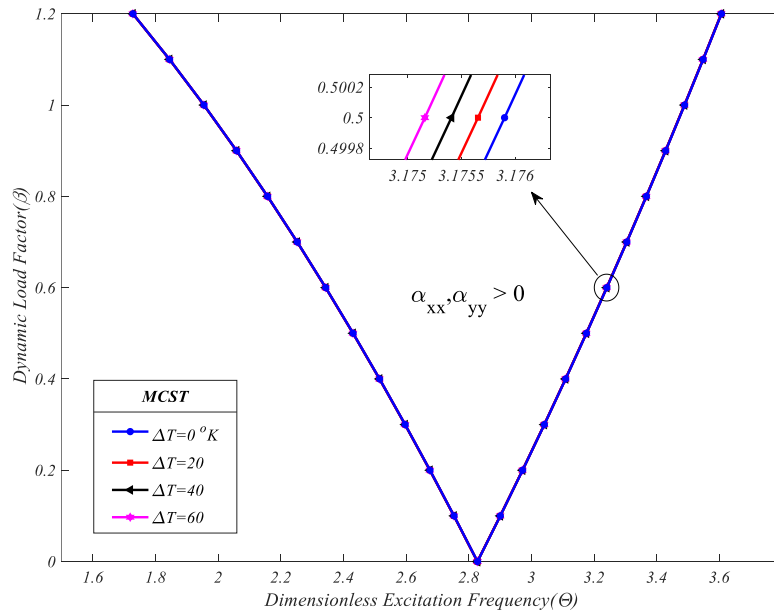


Fig 10: The effect of high temperature on the DIR

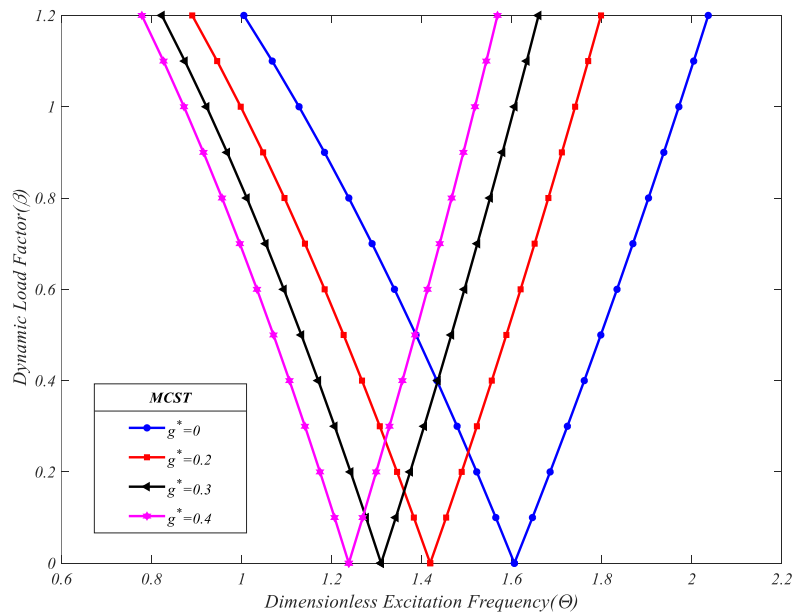


Fig 11: The effect of structural damping on the DIR

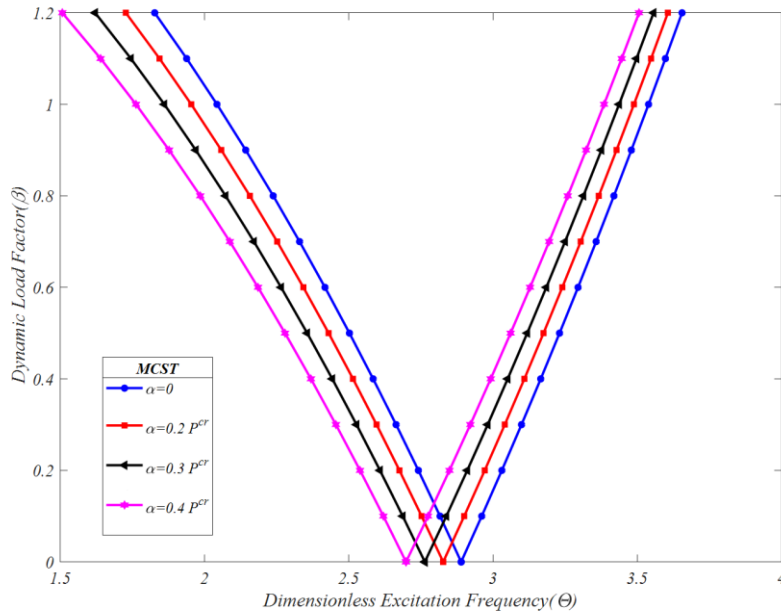


Fig 12: The effect of static load factor on the DIR

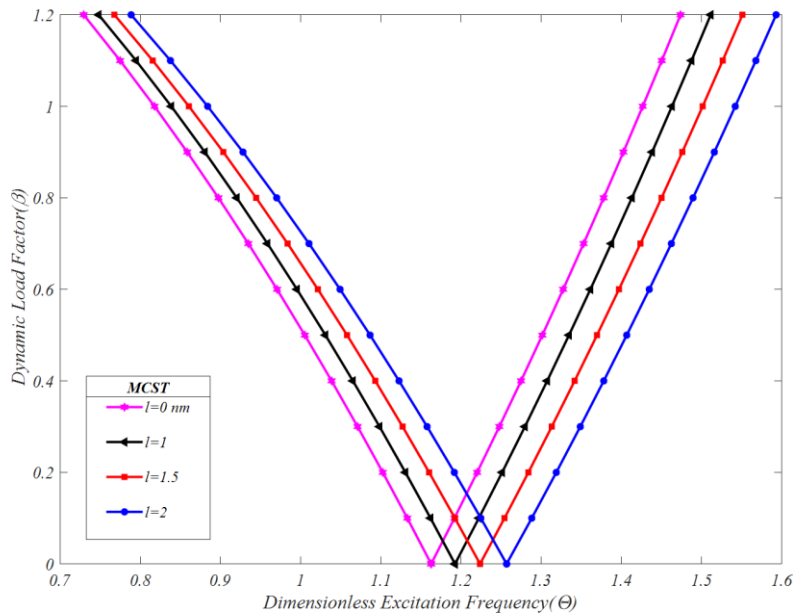


Fig 13: The effect of length scale parameter on the DIR

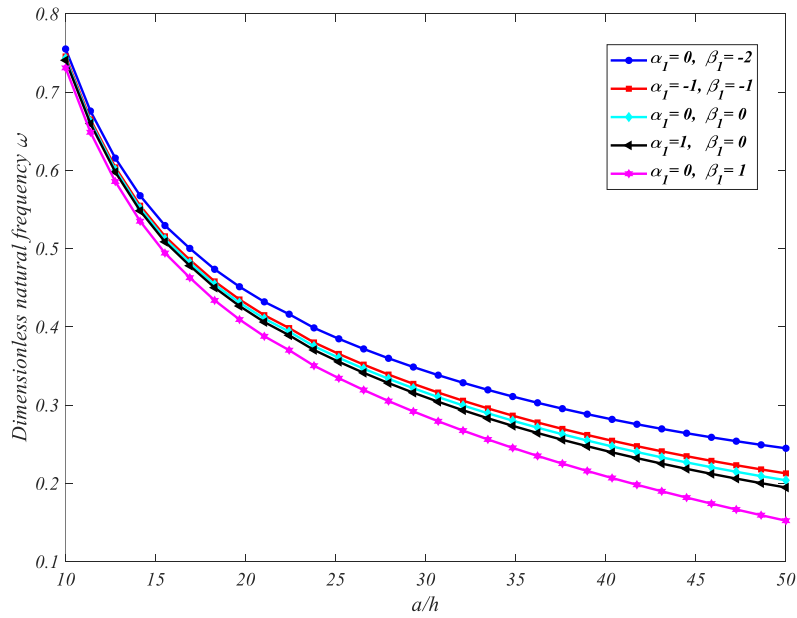


Fig 14: Impact of voltage on the dimensionless natural frequency versus aspect ratio

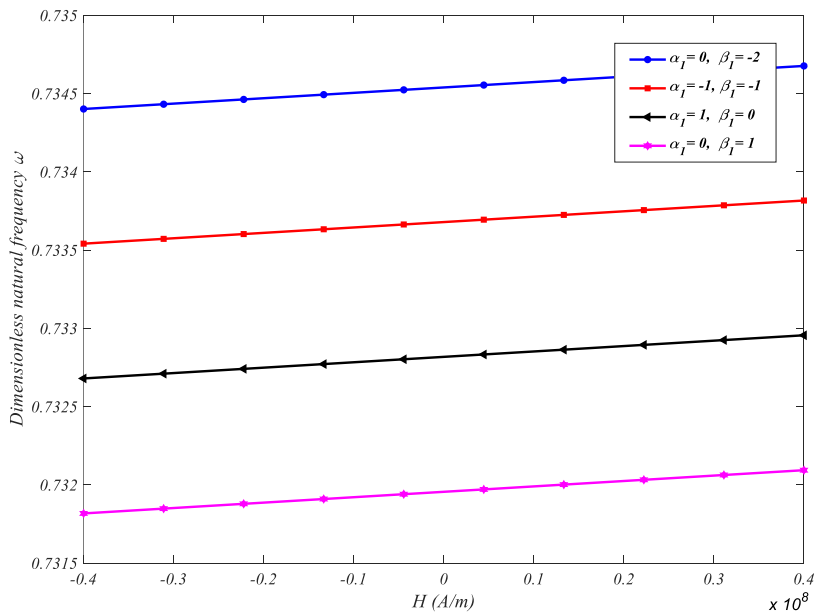


Fig 15: Impact of voltage on the dimensionless natural frequency versus magnetic field

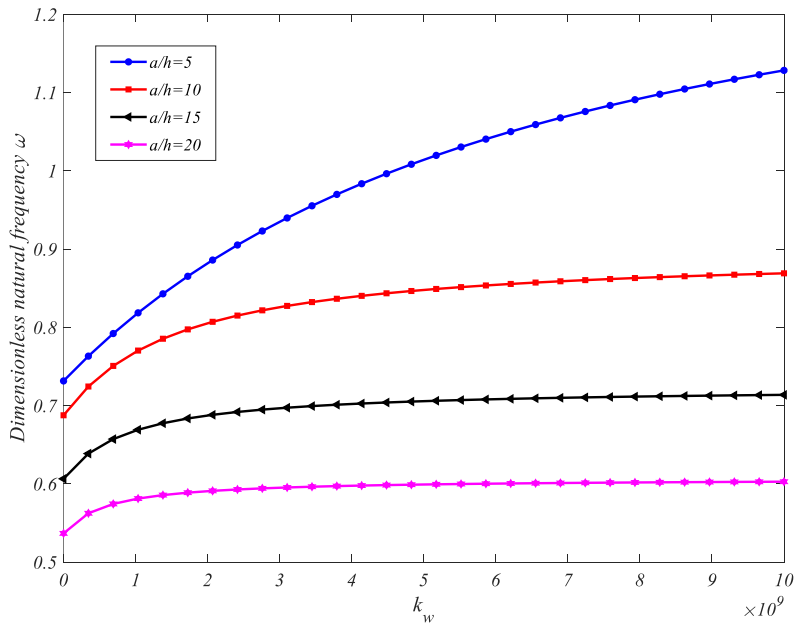


Fig 16: Impact of aspect ratio on the dimensionless natural frequency versus Winkler constant

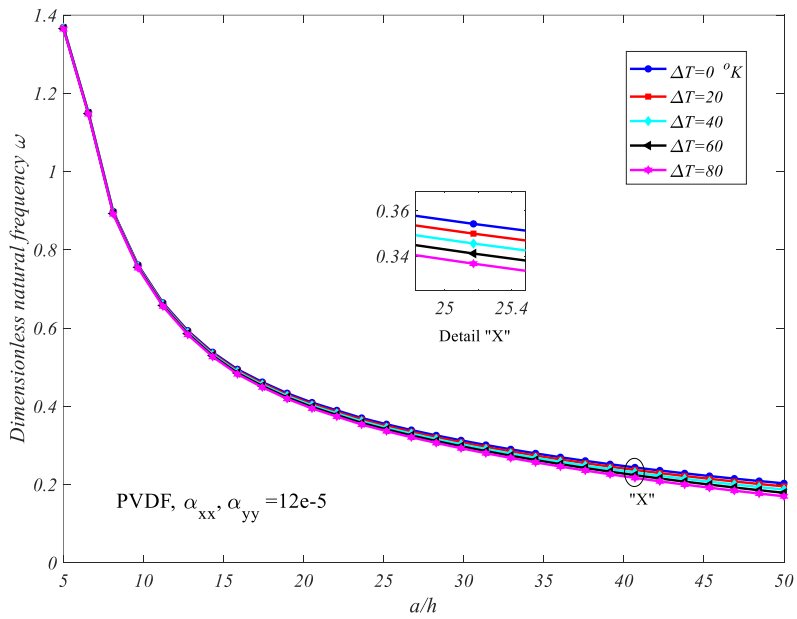


Fig 17: Impact of temperature on the dimensionless natural frequency versus aspect ratio

Acknowledgements

The authors would like to thank the referees for their valuable comments.

Appendix A.

$$m_{11} = -\frac{1}{4}\Lambda_{24}, m_{13} = -\frac{1}{4}\Lambda_{22}, m_{15} = -\frac{1}{4}m\pi(\Lambda_{20} - \Lambda_{21}), m_{22} = -\frac{1}{4}\zeta_6, m_{24} = -\frac{1}{4}\zeta_2, m_{25} = -\frac{1}{4}n\pi(\zeta_3 - \zeta_4), \quad (A1)$$

$$m_{31} = -\frac{1}{4}\theta_{70}, m_{33} = -\frac{1}{4}\theta_{69}, m_{35} = -\frac{1}{4}m\pi(\theta_{41} - \theta_{42}), m_{42} = -\frac{1}{4}\mathcal{G}_4, m_{44} = -\frac{1}{4}\mathcal{G}_3, m_{45} = -\frac{1}{4}n\pi(\mathcal{G}_{12} - \mathcal{G}_{13}), \quad (A2)$$

$$m_{51} = \frac{1}{4}m\pi(\varpi_3 - \varpi_4), m_{52} = \frac{1}{4}n\pi(\varpi_{11} - \varpi_{12}), m_{53} = \frac{1}{4}m\pi(\varpi_{73} - \varpi_{74}), m_{54} = \frac{1}{4}\pi(\varpi_{71} - \varpi_{72}), \quad (A3)$$

$$m_{55} = -\frac{1}{4}(m^2(\varpi_6 - \varpi_7 + \varpi_5) + n^2(\varpi_8 - \varpi_9 + \varpi_{10}))\pi^2 - \frac{1}{4}\varpi_{111}. \quad (A3)$$

$$k_8 = -\frac{1}{4}(m^2\varpi_2 + n^2\varpi_1)\pi^2, \varpi_2, \varpi_1 = \frac{h^2}{a^2}, \frac{h^2}{b^2}, \quad c_i^m = \alpha_2, \alpha_4, \alpha_6, \alpha_8, \alpha_{15}, i = 13, 23, 33, 43, 53 \quad (A4)$$

$$k'_{11} = -\frac{1}{4}((m^2n^2\Lambda_{35} + n^4\Lambda_8)\pi^2 + m^2(\Lambda_{14} + \Lambda_{25} - \Lambda_{39}) + \Lambda_9n^2)\pi^2, \quad k'_{12} = \frac{1}{4}m((m^2\Lambda_{34} + n^2\Lambda_{33})\pi^2 - \Lambda_{40} - \Lambda_{41})n\pi^2, \quad (A5)$$

$$k'_{13} = -\frac{1}{4}(n^2(m^2\Lambda_{32} + n^2\Lambda_{15})\pi^2 + (\Lambda_{16} + \Lambda_{17})n^2 + m^2(\Lambda_{18} + \Lambda_{19} - \Lambda_{29}))\pi^2, \quad (A6)$$

$$k'_{14} = \frac{1}{4}mn\pi^2((m^2\Lambda_{31} + n^2\Lambda_{30})\pi^2 - \Lambda_{26} - \Lambda_{27} + \Lambda_{28}), \quad (A7)$$

$$k'_{15} = \frac{1}{4}m\pi^3(m^2(\Lambda_{10} - \Lambda_{11} + \Lambda_{12} - \Lambda_{13} - \Lambda_{36} + \Lambda_{37}) - n^2(\Lambda_{42} - \Lambda_{43} - \Lambda_{44})), \quad (A8)$$

$$k'_{16} = \frac{1}{4}\pi m \Lambda_{61}, k'_{26} = \frac{1}{4}\pi n \zeta_{66}, \quad k'_{36} = \frac{1}{4}\pi m(\theta_{82} + \theta_{83}), \quad k'_{21} = \frac{1}{4}\pi^2 m((m^2\zeta_{56} + n^2\zeta_{55})\pi^2 - \zeta_{49} - \zeta_{50})n, \quad (A9)$$

$$k'_{22} = -\frac{1}{4}(m^2(m^2\zeta_{26} + n^2\zeta_{54})\pi^2 + m^2\zeta_{27} + n^2(\zeta_{32} - \zeta_{47} + \zeta_{67}))\pi^2, k'_{23} = \frac{1}{4}((m^2\zeta_{40} + n^2\zeta_{39})\pi^2 - \zeta_{41} - \zeta_{42} + \zeta_{43})\pi^2 mn, \quad (A10)$$

$$k'_{24} = -\frac{1}{4}\pi^2(m^2(m^2\zeta_{33} + n^2\zeta_{38})\pi^2 + (\zeta_{22} + \zeta_{23})m^2 + n^2(\zeta_{24} + \zeta_{25} - \zeta_{44})), \quad (A11)$$

$$k'_{25} = \frac{1}{4}\pi^3((\zeta_{51} + \zeta_{52} - \zeta_{53})m^2 + n^2(\zeta_{28} - \zeta_{29} + \zeta_{30} - \zeta_{31} - \zeta_{45} + \zeta_{46}))n, \quad (A12)$$

$$k'_{31} = -\frac{1}{4}(n^2(m^2\theta_{15} + n^2\theta_{50})\pi^2 + (\theta_{52} - \theta_{54} - \theta_2)m^2 + n^2(\theta_{53} + \theta_{57}))\pi^2, \quad (A13)$$

$$k'_{32} = \frac{1}{4}\pi^2((m^2\theta_{14} + n^2\theta_{22})\pi^2 - \theta_5 - \theta_6 + \theta_7)nm, \quad (A14)$$

$$k'_{33} = \frac{1}{4}(-m^2n^2\theta_{43} - n^4\theta_{62})\pi^4 + \frac{1}{4}((\theta_{51} - \theta_{63} - \theta_{65} - \theta_{68})m^2 - n^2(\theta_{64} + \theta_{66} + \theta_{67}))\pi^2 - \frac{1}{4}(\theta_{78} + \theta_{79}), \quad (A15)$$

$$k'_{34} = \frac{1}{4}n\pi^2((m^2\theta_{61} + n^2\theta_{60})\pi^2 - \theta_{55} - \theta_{56} + \theta_{58} + \theta_{59})m, \quad (A16)$$

$$k'_{35} = \frac{1}{4}m\pi \left(\left((\theta_{12} - \theta_{13} + \theta_{44} + \theta_{45} - \theta_{46} - \theta_{47} + \theta_{48} - \theta_{49})m^2 \right) \right. \\ \left. + n^2(\theta_{16} + \theta_{17} + \theta_{18} - \theta_{19} - \theta_{20} - \theta_{21}) \right) \pi^2 - \theta_{26} + \theta_{27} - \theta_{28}, \quad (A17)$$

$$k'_{41} = \frac{1}{4}n\pi^2((m^2\mathcal{G}_{78} + n^2\mathcal{G}_{77})\pi^2 - \mathcal{G}_{17} - \mathcal{G}_{18} + \mathcal{G}_{19})m, \quad (A18)$$

$$k'_{42} = -\frac{1}{4}(m^2(m^2\mathcal{G}_{47} + n^2\mathcal{G}_{76})\pi^2 + (-\mathcal{G}_{16} + \mathcal{G}_{49} - \mathcal{G}_{50})n^2 + m^2(\mathcal{G}_{55} + \mathcal{G}_{36}))\pi^2, \quad (A19)$$

$$k'_{43} = \frac{1}{4}n((m^2\mathcal{G}_{48} + n^2\mathcal{G}_{46})\pi^2 + \mathcal{G}_{37} - \mathcal{G}_{38} - \mathcal{G}_{39} - \mathcal{G}_{40})\pi^2 m, \quad (A20)$$

$$k'_{44} = \frac{1}{4}(-m^4\mathcal{G}_9 - m^2n^2\mathcal{G}_{45})\pi^4 + \frac{1}{4}((-\mathcal{G}_8 - \mathcal{G}_{10} - \mathcal{G}_{11} + \mathcal{G}_{53})n^2 - m^2(\mathcal{G}_5 + \mathcal{G}_6 - \mathcal{G}_7))\pi^2 - \frac{1}{4}(\mathcal{G}_{33} + \mathcal{G}_{34}), \quad (A21)$$

$$k'_{45} = -\frac{1}{4}n \left(\left((-\mathcal{G}_{41} + \mathcal{G}_{42} - \mathcal{G}_{43} - \mathcal{G}_{44} + \mathcal{G}_{51} + \mathcal{G}_{52} - \mathcal{G}_{82} + \mathcal{G}_{83})n^2 \right) \right. \\ \left. + m^2(\mathcal{G}_{73} - \mathcal{G}_{74} - \mathcal{G}_{75} + \mathcal{G}_{79} + \mathcal{G}_{80} - \mathcal{G}_{81}) \right) \pi^2 - \mathcal{G}_{30} + \mathcal{G}_{31} + \mathcal{G}_{32}, \quad (A22)$$

$$k'_{46} = \frac{1}{4}\pi n(\mathcal{G}_{34} + \mathcal{G}_{35}), \quad k'_{56} = -\frac{1}{4}\pi^2(m^2\varpi_{139} + n^2\varpi_{153}), \quad (A23)$$

$$k'_{51} = -\frac{1}{4}((\varpi_{52} - \varpi_{53} - \varpi_{97} - \varpi_{98} + \varpi_{99})m^2 - n^2(\varpi_{31} + \varpi_{32}))m\pi^3, \tag{A24}$$

$$k'_{52} = \frac{1}{4}n\pi^3((\varpi_{29} + \varpi_{30})m^2 - n^2(\varpi_{34} - \varpi_{35} - \varpi_{107} - \varpi_{108} + \varpi_{109})), \tag{A25}$$

$$k'_{53} = -\frac{1}{4}m\pi^3((\varpi_{38} - \varpi_{39} - \varpi_{89} + \varpi_{90} - \varpi_{91} - \varpi_{92})m^2 - n^2(\varpi_{43} + \varpi_{44} + \varpi_{45})), \tag{A26}$$

$$k'_{54} = \frac{1}{4}n\pi^3((\varpi_{40} + \varpi_{41} + \varpi_{42})m^2 - n^2(\varpi_{36} - \varpi_{37} - \varpi_{85} + \varpi_{86} - \varpi_{87} - \varpi_{88})), \tag{A27}$$

$$k'_{55} = \frac{1}{4} \left(\begin{aligned} & \left((\varpi_{106} - \varpi_{105} + \varpi_{104} - \varpi_{82} - \varpi_{58} + \varpi_{83} + \varpi_{57} - \varpi_{84} + \varpi_{59} - \varpi_{103})m^4 \right) \\ & - n^2(\varpi_{24} + \varpi_{25} - \varpi_{26} + \varpi_{27} - \varpi_{28})m^2 \\ & + n^4(\varpi_{54} - \varpi_{55} + \varpi_{56} - \varpi_{75} + \varpi_{76} - \varpi_{77} - \varpi_{78} + \varpi_{79} - \varpi_{80} + \varpi_{81}) \\ & + (\varpi_{122} + \varpi_{123} + \varpi_{124} + \varpi_{125} - \varpi_{13} + \varpi_{14} + \varpi_{15} - \varpi_{16} - \varpi_{17} - \varpi_{93} - \varpi_{94})m^2 \\ & + (\varpi_{126} + \varpi_{127} + \varpi_{128} + \varpi_{129} + \varpi_{62} - \varpi_{63} - \varpi_{64} - \varpi_{65} - \varpi_{95} - \varpi_{96})n^2 \end{aligned} \right) \pi^2, \tag{A28}$$

$$k'_{63} = -\frac{1}{4}\pi m(\eta_9 + \eta_2), \quad k'_{64} = -\frac{1}{4}\pi n(\eta_{12} + \eta_5), \tag{A29}$$

$$k'_{65} = -\frac{1}{4}\pi^2((\eta_1 - \eta_7 + \eta_8)m^2 + n^2(\eta_4 - \eta_{10} + \eta_{11})), \tag{A30}$$

$$k'_{66} = \frac{1}{4}(-\eta_3 m^2 - \eta_6 n^2)\pi^2 - \frac{1}{4}\eta_{13}. \tag{A31}$$

$$\alpha_1 = -\frac{1}{9n} \left(8 \left(\Lambda_{52} - \frac{1}{2}(\Lambda_{55} + \Lambda_{56}) \right) n^2 + 8m^2(\Lambda_{38} + \Lambda_{23}) \right) \pi, \tag{A32}$$

$$\alpha_2 = \frac{1}{9n} (4(\Lambda_1 + \Lambda_2 + \Lambda_3 + \Lambda_4) - 8(\Lambda_5 + \Lambda_6))n^2 - 8m^2(\Lambda_{48} + \Lambda_{49}), \tag{A33}$$

$$\alpha_3 = -\frac{1}{9m} \left(8 \left(\zeta_7 - \frac{1}{2}(\zeta_{13} + \zeta_{14}) \right) m^2 + 8n^2(\zeta_{48} + \zeta_1) \right) \pi, \tag{A34}$$

$$\alpha_4 = \frac{1}{9m} (-8(\zeta_{15} + \zeta_{16}) + 4(\zeta_{17} + \zeta_{18} + \zeta_{19} + \zeta_{20}))m^2 - 8n^2(\zeta_{36} + \zeta_{37}), \tag{A35}$$

$$\alpha_5 = -\frac{8\pi}{9n} 8\pi \left(\left(-\frac{1}{2}(\theta_{38} + \theta_{39}) + \theta_{40} \right) n^2 + m^2(\theta_{24} + \theta_{25}) \right), \tag{A36}$$

$$\alpha_6 = -\frac{1}{9n} \left(8 \left(\theta_{73} + \theta_{74} - \frac{1}{2}(\theta_{75} + \theta_{76} + \theta_{77} + \theta_{72}) \right) n^2 + 8m^2(\theta_{84} + \theta_{85}) \right) \pi, \tag{A37}$$

$$\alpha_7 = -\frac{8\pi}{9m} \left(\left(\varrho_{57} - \frac{1}{2}(\varrho_{59} + \varrho_{60}) \right) m^2 + n^2(\varrho_{71} + \varrho_{72}) \right), \tag{A38}$$

$$\alpha_8 = \frac{1}{9m} (-8(\varrho_1 + \varrho_2) + 4(\varrho_{26} + \varrho_{27} + \varrho_{28} + \varrho_{29}))m^2 - 8n^2(\varrho_{25} + \varrho_{69}), \tag{A39}$$

$$\alpha_{9,12} = \frac{16}{9n}\varpi_{70}m^2\pi, \frac{16}{9m}\varpi_{61}n^2\pi, \frac{16}{9n}\varpi_{69}m^2\pi, \frac{16}{9m}\varpi_{60}n^2\pi, \tag{A40}$$

$$\alpha_{13} = \frac{1}{9}nm \left(\begin{aligned} & 16 \left(\varpi_{101} - \frac{1}{2} \left(\varpi_{21} - \varpi_{22} + \frac{1}{2} \varpi_{23} \right) \right) m^4 \\ & + 4n^2 \left(4\varpi_{121} - 2(\varpi_{130} + \varpi_{131} + \varpi_{132} + \varpi_{133}) + \varpi_{66} + \varpi_{67} \right) m^2 \\ & + 16n^4 \left(\varpi_{100} + \frac{1}{2}(\varpi_{19} - \varpi_{20} - \varpi_{33}) \right) \end{aligned} \right) \pi^2, \tag{A41}$$

$$\alpha_{14,15} = \frac{1}{64}(-3m^4\varpi_{68} - 3n^4\varpi_{18})\pi^4 - \frac{9}{64}\varpi_{102}, -2n^4 \left(\varpi_{136} - \frac{1}{2}(\varpi_{137} + \varpi_{141}) \right). \tag{A42}$$

$$c'_{11} = -\frac{1}{4}\pi^2(m^2\Lambda_7 + n^2\Lambda_{58}), \quad c'_{12} = -\frac{1}{4}m\pi^2n(\Lambda_{64} + \Lambda_{65}), c'_{13} = -\frac{1}{4}\pi^2(m^2\Lambda_{46} + n^2\Lambda_{47}), \tag{A43}$$

$$c'_{14} = -\frac{1}{4}m\pi^2n(\Lambda_{53} + \Lambda_{54}), \quad c'_{15} = \frac{1}{4}((-\Lambda_{62} - \Lambda_{63} + \Lambda_{66} + \Lambda_{67})n^2 + m^2(\Lambda_{50} - \Lambda_{51}))m\pi^3, \tag{A44}$$

$$c'_{21} = -\frac{1}{4}m\pi^2n(\zeta_{60} + \zeta_{63}), \quad c'_{22} = -\frac{1}{4}\pi^2(m^2\zeta_5 + n^2\zeta_{21}), c'_{23} = -\frac{1}{4}m\pi^2n(\zeta_{34} + \zeta_{35}), \tag{A45}$$

$$c'_{24} = -\frac{1}{4}\pi^2(m^2\zeta_{57} + n^2\zeta_{58}), \quad c'_{25} = -\frac{1}{4}\pi^3((-\zeta_{10} + \zeta_{11})n^2 + (\zeta_{61} - \zeta_{62} + \zeta_{64} - \zeta_{65})m^2)n, \tag{A46}$$

$$c'_{31} = -\frac{1}{4}\pi^2(m^2\theta_8 + n^2\theta_{11}), \quad c'_{32} = -\frac{1}{4}\pi^2 mn(\theta_{31} + \theta_{35}), \quad c'_{33} = -\frac{1}{4}(m^2\theta_{33} + n^2\theta_{29})\pi^2 - \frac{1}{4}\theta_{71}, \quad (A47)$$

$$c'_{34} = -\frac{1}{4}\pi^2 mn(\theta_{80} + \theta_{81}), \quad c'_{35} = \frac{1}{4}m\pi(((\theta_9 - \theta_{10})m^2 + n^2(\theta_{32} - \theta_{34} + \theta_{36} - \theta_{37}))\pi^2 - \theta_{23}), \quad (A48)$$

$$c'_{41} = -\frac{1}{4}m\pi^2 n(\varrho_{61} + \varrho_{65}), \quad c'_{42} = -\frac{1}{4}\pi^2(m^2\varrho_{15} + n^2\varrho_{84}), \quad c'_{43} = -\frac{1}{4}m\pi^2 n(\varrho_{24} + \varrho_{70}), \quad (A49)$$

$$c'_{44} = -\frac{1}{4}(m^2\varrho_{68} + n^2\varrho_{63})\pi^2 - \frac{1}{4}\varrho_{56}, \quad c'_{45} = \frac{1}{4}n\pi(((-\varrho_{14} + \varrho_{85})n^2 + m^2(\varrho_{62} - \varrho_{64} + \varrho_{66} - \varrho_{67}))\pi^2 - \varrho_{20}), \quad (A50)$$

$$c'_{51} = \frac{1}{4}\pi^3 m(m^2\varpi_{120} + n^2(B_{12}\varpi_{143} + \varpi_{144})), \quad c'_{52} = \frac{1}{4}\pi^3((\varpi_{145} + \varpi_{146})m^2 + \varpi_{175}n^2)n, \quad (A51)$$

$$c'_{53} = \frac{1}{4}\pi^3 m(m^2\varpi_{47} + n^2(\varpi_{114} + \varpi_{119})), \quad c'_{54} = \frac{1}{4}\pi^3((\varpi_{113} + \varpi_{118})m^2 + \varpi_{46}n^2)n, \quad (A52)$$

$$c'_{55} = \frac{1}{4}((-\varpi_{117} + \varpi_{165})m^4 - n^2(\varpi_{147} + \varpi_{148} - \varpi_{149} - \varpi_{150})m^2 + n^4(\varpi_{115} - \varpi_{116}))\pi^4 - \frac{1}{4}\varpi_{112}. \quad (A53)$$

Appendix B.

$$\Lambda_{1..7} = \left(\frac{I_0}{A_{11}}\right)^{-0.5} \left(\frac{h^2 g A_{12}}{A_{11} b^2 a}, \frac{h^2 g A_{12}}{A_{11} b^2 a}, \frac{h g}{a^2}\right), \quad (B1)$$

$$\Lambda_{8..20} = \frac{1}{8} \frac{h^2 P_1}{A_{11} b^4}, \frac{h^2 A_{66}}{A_{11} b^3}, -\frac{h^2 A_3}{A_{11} a^3}, \frac{h^2 A_4}{A_{11} a^3}, -\frac{h^2 B_{11}}{A_{11} a^3}, \frac{h^2 C_{11}}{A_{11} a^2}, \frac{h^2 A_1}{A_{11} a^2}, -\frac{1}{8} \frac{h P_2}{A_{11} b}, \frac{h C_{66}}{A_{11} b^2}, \frac{1}{8} \frac{h P_5}{A_{11} b^2}, \frac{h A_4}{A_{11} a^2}, \frac{h C_{11}}{A_{11} a^2}, -\frac{I_3}{a I_0}, \quad (B2)$$

$$\Lambda_{21..32} = \frac{I_1}{a I_0}, -\frac{I_3}{h I_0}, \frac{h^3}{a^3}, -1, \frac{h^2}{a^2}, \frac{h C_{12}}{A_{11} b a}, \frac{h C_{66}}{A_{11} b a}, -\frac{1}{8} \frac{h P_5}{A_{11} b a}, -\frac{h C^2 I_3}{A_{11} a^2}, \frac{1}{8} \frac{h P_2}{A_{11} b^3 a}, \frac{1}{8} \frac{h P_2}{A_{11} b a^3}, -\frac{1}{8} \frac{h P_2}{A_{11} b^2 a^2}, \quad (B3)$$

$$\Lambda_{33..43} = \frac{1}{8} \frac{h^2 P_1}{A_{11} b^3 a}, \frac{1}{8} \frac{h^2 P_1}{A_{11} b a^3}, -\frac{1}{8} \frac{h^2 P_1}{A_{11} b^2 a^2}, \frac{h^2 C^2 I_1}{A_{11} a^3}, -\frac{h^2 C^2 I_3}{A_{11} a^3}, \frac{h^3 A_1}{A_{11} a^3}, -\frac{h^2 C^2 I_0}{A_{11} a^2}, \frac{h^2 A_{12}}{A_{11} b a}, \frac{h^2 A_{66}}{A_{11} b^2 a}, \frac{h^2 C_{12}}{A_{11} b^2 a}, -\frac{h^2 B_{12}}{A_{11} b^2 a}, \quad (B4)$$

$$\Lambda_{44..67} = -2 \frac{h^2 B_{66}}{A_{11} b^2 a}, \left(\frac{I_0}{A_{11}}\right)^{-0.5} \left(-2 \frac{C I_3}{A_{11} a}, \frac{C_{11} g}{A_{11} a^2}, \frac{C_{66} g}{A_{11} b^2}, \frac{h^2 g}{a^3}, \frac{h^2 g}{a^3}, -\frac{h g B_{11}}{A_{11} a^3}, \frac{h g C_{11}}{A_{11} a^3}\right), \frac{h^3 A_{66}}{A_{11} b^2 a}, \quad (B5)$$

$$\left(\frac{I_0}{A_{11}}\right)^{-0.5} \left(\frac{g C_{12}}{A_{11} b a}, \frac{C_{66} g}{A_{11} b a}\right), \frac{h^3 A_2}{A_{11} b^2 a}, \frac{h^3 A_{66}}{A_{11} b^2 a}, \left(\frac{I_0}{A_{11}}\right)^{-0.5} \left(-2 \frac{h C I_0}{A_{11} a}, \frac{h A_{66} g}{A_{11} b^2}, 2 \frac{h C I_1}{A_{11} a^2}, -2 \frac{h C I_3}{A_{11} a^2}\right), \quad (B5)$$

$$\frac{h^2 e_{31} A_{77} e_{15}}{A_{11} a \xi_{11}}, \left(\frac{I_0}{A_{11}}\right)^{-0.5} \left(-\frac{h g B_{12}}{A_{11} b^2 a}, -2 \frac{h g B_{66}}{A_{11} b^2 a}, \frac{h A_{66} g}{A_{11} b a}, \frac{h g A_{12}}{A_{11} b^2 a}, \frac{h g C_{12}}{A_{11} b^2 a}, 2 \frac{h g C_{66}}{A_{11} b^2 a}\right). \quad (B5)$$

$$\zeta_{1..7} = \frac{h^3}{b^3}, -\frac{I_3}{h I_0}, \frac{I_1}{b I_0}, -\frac{I_3}{b I_0}, \left(\frac{I_0}{A_{11}}\right)^{-0.5} \frac{h A_{66} g}{A_{11} a^2}, -1, \frac{h^3 A_{66}}{A_{11} a^2 b}, 2 \left(\frac{I_0}{A_{11}}\right)^{-0.5} \frac{h C I_1}{A_{11} b^2}, \quad (B6)$$

$$\zeta_{8..20} = \left(\frac{I_0}{A_{11}}\right)^{-0.5} \left(2 \frac{h C I_1}{A_{11} b^2}, -2 \frac{h C I_3}{A_{11} b^2}, -\frac{h g B_{11}}{A_{11} b^3}, \frac{h g C_{11}}{A_{11} b^3}, -2 \frac{h C I_0}{A_{11} b}\right), \frac{h^3 A_2}{A_{11} b a^2}, \frac{h^3 A_{66}}{A_{11} b a^2}, \quad (B7)$$

$$\left(\frac{I_0}{A_{11}}\right)^{-0.5} \left(\frac{h^2 A_{66} g}{A_{11} b a^2}, \frac{h^2 A_{66} g}{A_{11} b a^2}, \frac{h^2 A_{66} g}{A_{11} b a^2}, \frac{h^2 A_{12} g}{A_{11} b a^2}, \frac{h^2 A_{66} g}{A_{11} b a^2}, \frac{h^2 A_{12} g}{A_{11} b a^2}\right), \quad (B7)$$

$$\zeta_{21..32} = \left(\frac{I_0}{A_{11}}\right)^{-0.5} \frac{h g}{b^2}, \frac{h C_{66}}{A_{11} a^2}, \frac{1}{8} \frac{h P_5}{A_{11} a^2}, \frac{h A_4}{A_{11} b^2}, \frac{h C_{11}}{A_{11} b^2}, -\frac{1}{8} \frac{h^2 P_1}{A_{11} a^4}, \frac{h^2 A_{66}}{A_{11} a^2}, \frac{h^2 A_2}{A_{11} b^3}, \frac{h^2 A_4}{A_{11} b^3}, -\frac{h^2 B_{11}}{A_{11} b^3}, \frac{h^2 C_{11}}{A_{11} b^3}, \frac{h^2 A_1}{A_{11} b^2}, \quad (B8)$$

$$\zeta_{33..43} = -\frac{1}{8} \frac{h P_2}{A_{11} a^4}, \left(\frac{I_0}{A_{11}}\right)^{-0.5} \left(\frac{g C_{12}}{A_{11} b a}, \frac{g C_{66}}{A_{11} b a}, \frac{h^2 g}{b^3}, \frac{h^2 g}{b^3}\right), -\frac{1}{8} \frac{h P_2}{A_{11} b^2 a^2}, \frac{1}{8} \frac{h P_2}{A_{11} b^3 a}, \frac{1}{8} \frac{h P_2}{A_{11} b a^3}, \frac{h C_{12}}{A_{11} b a}, \frac{h C_{66}}{A_{11} b a}, -\frac{1}{8} \frac{h P_5}{A_{11} b a}, \quad (B9)$$

$$\zeta_{44..67} = -\frac{h C^2 I_3}{A_{11} b^2}, \frac{h^2 C^2 I_1}{A_{11} b^3}, -\frac{h^2 C^2 I_3}{A_{11} b^3}, -\frac{h^2 C^2 I_0}{A_{11} b^2}, \frac{h^3 A_1}{A_{11} b^3}, \frac{h^2 A_{66}}{A_{11} b a}, \frac{h^2 A_{12}}{A_{11} b a}, -\frac{h^2 B_{12}}{A_{11} b a^2}, -2 \frac{h^2 B_{66}}{A_{11} b a^2}, \frac{h^2 C_{12}}{A_{11} b a^2}, -\frac{1}{8} \frac{h^2 P_1}{A_{11} b^2 a^2}, \quad (B9)$$

$$\frac{1}{8} \frac{h^2 P_1}{A_{11} b^3 a}, \frac{1}{8} \frac{h^2 P_1}{A_{11} b a^3}, \left(\frac{I_0}{A_{11}}\right)^{-0.5} \left(\frac{C_{66} g}{A_{11} a^2}, \frac{C_{11} g}{A_{11} b^2}, -2 \frac{C I_3}{A_{11} b}, \frac{h g A_{66}}{A_{11} b a}, \frac{h g C_{12}}{A_{11} b a^2}, -\frac{h g B_{12}}{A_{11} b a^2}, \frac{h g A_{12}}{A_{11} b a}, 2 \frac{h g C_{66}}{A_{11} b a^2}, -2 \frac{h g B_{66}}{A_{11} b a^2}\right), \quad (B10)$$

$$\frac{h^2 e_{32} A_{77} e_{15}}{A_{11} b \xi_{11}}, \frac{h^2}{b^2}. \quad (B10)$$

$$\theta_{1..7} = -2 \left(\frac{I_0}{A_{11}}\right)^{-0.5} \frac{C I_5}{A_{11} a^2}, -\frac{h C^2 I_3}{A_{11} a^2}, \left(\frac{I_0}{A_{11}}\right)^{-0.5} \left(-2 \frac{C I_3}{A_{11} a}, 2 \frac{C I_4}{A_{11} a^2}\right), \frac{h C_{12}}{A_{11} b a}, \frac{h C_{66}}{A_{11} b a}, -\frac{1}{8} \frac{h P_5}{A_{11} b a}, \quad (B11)$$

$$\theta_{8.20} = \left(\frac{I_0}{A_1} \right)^{-0.5} \left(\frac{C_{11}g}{A_1a^2}, -\frac{E_{11}g}{A_1a^3}, \frac{F_{11}g}{A_1a^3}, \frac{C_{66}g}{A_1b^2} \right), -\frac{C^2I_5h}{A_1a^3}, \frac{C^2I_4h}{A_1a^3}, \frac{1}{8} \frac{P_2h}{A_1ba^3}, -\frac{1}{8} \frac{P_2h}{A_1b^2a^2}, -\frac{E_{12}h}{A_1b^2a},$$

$$-2 \frac{E_{66}h}{A_1b^2a}, -\frac{1}{4} \frac{P_{24}h}{A_1b^2a}, \frac{F_{12}h}{A_1b^2a}, 2 \frac{F_{66}h}{A_1b^2a}, \quad (B12)$$

$$\theta_{21.32} = \frac{1}{8} \frac{P_2h}{A_1b^3a}, \frac{1}{8} \frac{P_2h}{A_1b^3a}, -\left(\frac{I_0}{A_1} \right)^{-0.5} \frac{gA_{55}}{A_1a}, \frac{A_4h^2}{A_1a^3}, \frac{C_{11}h^2}{A_1a^3}, -\frac{A_{55}h}{A_1a}, \frac{B_2h}{A_1a}, \frac{1}{8} \frac{P_{10}h}{A_1a}, \left(\frac{I_0}{A_1} \right)^{-0.5} \frac{F_{66}g}{A_1b^2h},$$

$$\left(\frac{I_0}{A_1} \right)^{-0.5} \left(-2 \frac{CI_5}{A_1ah}, \frac{C_{12}g}{A_1ba}, -\frac{E_{12}g}{A_1b^2a} \right), \quad (B13)$$

$$\theta_{33.43} = \left(\frac{I_0}{A_1} \right)^{-0.5} \left(\frac{F_{11}g}{A_1a^2h}, \frac{F_{12}g}{A_1b^2a}, \frac{C_{66}g}{A_1ba}, -2 \frac{E_{66}g}{A_1b^2a}, 2 \frac{F_{66}g}{A_1b^2a} \right), \frac{C_{12}h^2}{A_1b^2a}, \frac{C_{66}h^2}{A_1b^2a}, \frac{C_{66}h^2}{A_1b^2a}, -\frac{I_5}{ahI_0}, \frac{I_4}{ahI_0}, -\frac{1}{8} \frac{P_3}{A_1b^2a^2},$$

$$\quad (B14)$$

$$\theta_{44.67} = -\frac{E_{11}h}{A_1a^3}, -\frac{A_5h}{A_1a^3}, \frac{F_{11}h}{A_1a^3}, \frac{A_6h}{A_1a^3}, -\frac{1}{4} \frac{P_4h}{A_1a^3}, \frac{1}{8} \frac{P_9h}{A_1a^3}, -\frac{1}{8} \frac{P_2h}{A_1b^4}, -\frac{C^2I_5}{A_1a^2}, \frac{C_{11}h}{A_1a^2}, \frac{C_{66}h}{A_1b^2},$$

$$-\frac{A_4h}{A_1a^2}, \frac{F_{12}}{A_1ba}, \frac{F_{66}}{A_1ba}, \frac{1}{8} \frac{P_5h}{A_1b^2}, -\frac{1}{4} \frac{P_6}{A_1ba}, -\frac{3}{8} \frac{P_9}{A_1ba}, \frac{1}{8} \frac{P_3}{A_1b^2a}, \frac{1}{8} \frac{P_3}{A_1ba^3}, -\frac{1}{8} \frac{P_3}{A_1b^4}, \frac{F_{11}}{A_1a^2}, \frac{F_{66}}{A_1b^2},$$

$$\frac{A_6}{A_1a^2}, \frac{1}{4} \frac{P_6}{A_1b^2}, \frac{1}{2} \frac{P_9}{A_1b^2}, \quad (B15)$$

$$\theta_{68.85} = \frac{1}{8} \frac{P_9}{A_1a^2}, -\frac{I_5}{h^2I_0}, -\frac{I_3}{hI_0}, \left(\frac{I_0}{A_1} \right)^{-0.5} \left(-\frac{gA_{55}}{A_1h}, \frac{C_{66}hg}{A_1b^2a}, \frac{C_{66}hg}{A_1b^2a}, \frac{C_{66}hg}{A_1b^2a}, \frac{C_{12}hg}{A_1b^2a}, \frac{C_{12}hg}{A_1b^2a}, \frac{C_{66}hg}{A_1b^2a} \right),$$

$$-\frac{1}{8} \frac{P_{10}}{A_1}, -\frac{A_{55}}{A_1}, \left(\frac{I_0}{A_1} \right)^{-0.5} \left(\frac{F_{66}g}{A_1bah}, \frac{F_{12}g}{A_1bah} \right), \frac{D_{77}e_{15}^2h}{A_1a\xi_{11}}, \frac{e_{31}C_{77}e_{15}h}{A_1a\xi_{11}}, \left(\frac{I_0}{A_1} \right)^{-0.5} \left(\frac{C_{11}hg}{A_1a^3}, \frac{C_{11}hg}{A_1a^3} \right).$$

$$\quad (B16)$$

$$\vartheta_{1.7} = \left(\frac{I_0}{A_1} \right)^{-0.5} \left(\frac{hgC_{66}}{A_1ba^2}, \frac{hgC_{66}}{A_1ba^2} \right), -\frac{I_5}{h^2I_0}, -\frac{I_3}{hI_0}, \frac{1}{4} \frac{P_6}{A_1a^2}, \frac{F_{66}}{A_1a^2}, -\frac{1}{2} \frac{P_9}{A_1a^2},$$

$$\quad (B17)$$

$$\vartheta_{8.20} = \frac{1}{8} \frac{P_9}{A_1b^2}, \frac{1}{8} \frac{P_3}{A_1a^2}, \frac{A_6}{A_1b^2}, \frac{F_{11}}{A_1b^2}, -\frac{I_5}{bhI_0}, \frac{I_4}{bhI_0}, \left(\frac{I_0}{A_1} \right)^{-0.5} \left(\frac{F_{11}g}{A_1b^3}, \frac{C_{66}g}{A_1a^2} \right), -\frac{hC^2I_3}{A_1b^2},$$

$$\frac{C_{12}h}{A_1ba}, \frac{C_{66}h}{A_1ba}, -\frac{1}{8} \frac{P_5h}{A_1ba}, -\left(\frac{I_0}{A_1} \right)^{-0.5} \frac{gA_{44}}{A_1b},$$

$$\quad (B18)$$

$$\vartheta_{21.32} = \left(\frac{I_0}{A_1} \right)^{-0.5} \left(-2 \frac{CI_5}{A_1b^2}, 2 \frac{CI_4}{A_1b^2}, -2 \frac{CI_3}{A_1b}, \frac{F_{12}g}{A_1bah}, \frac{C_{11}hg}{A_1b^3}, \frac{C_{12}hg}{A_1ba^2}, \frac{C_{12}hg}{A_1ba^2}, \frac{hgC_{66}}{A_1ba^2}, \frac{hgC_{66}}{A_1ba^2} \right), \frac{B_2h}{A_1b}, \frac{1}{8} \frac{P_{10}h}{A_1b}, -\frac{A_{44}h}{A_1b},$$

$$\quad (B19)$$

$$\vartheta_{33.43} = -\frac{1}{8} \frac{P_{10}}{A_1}, -\frac{A_{44}}{A_1}, \frac{C_{66}h}{A_1a^2}, \frac{1}{8} \frac{P_5h}{A_1a^2}, -\frac{1}{4} \frac{P_6}{A_1ba}, \frac{F_{12}}{A_1ba}, \frac{F_{66}}{A_1ba}, \frac{1}{8} \frac{P_9}{A_1ba}, -\frac{1}{4} \frac{P_4h}{A_1b^3}, \frac{1}{8} \frac{P_9h}{A_1b^3}, -\frac{A_5h}{A_1b^3},$$

$$\quad (B20)$$

$$\vartheta_{44.67} = -\frac{E_{11}h}{A_1b^3}, -\frac{1}{8} \frac{P_3}{A_1b^2a^2}, \frac{1}{8} \frac{P_3}{A_1b^3a}, -\frac{1}{8} \frac{P_2h}{A_1a^4}, \frac{1}{8} \frac{P_3}{A_1ba^3}, \frac{C_{11}h}{A_1b^2}, -\frac{A_4h}{A_1b^2}, \frac{A_6h}{A_1b^3}, \frac{F_{11}h}{A_1b^3}, -\frac{C^2I_5}{A_1b^2}, \frac{e_{32}C_{77}e_{15}h}{A_1b\xi_{11}},$$

$$\frac{D_{77}e_{24}e_{15}h}{A_1b\xi_{11}}, -\left(\frac{I_0}{A_1} \right)^{-0.5} \frac{gA_{44}}{A_1h}, 2 \frac{C_{66}h^2}{A_1ba^2}, -2 \left(\frac{I_0}{A_1} \right)^{-0.5} \frac{CI_5}{A_1bh}, \frac{h^2C_{12}}{A_1ba^2}, \frac{C_{66}h^2}{A_1ba^2},$$

$$\quad (B21)$$

$$\left(\frac{I_0}{A_1} \right)^{-0.5} \left(\frac{C_{12}g}{A_1ba}, -\frac{E_{12}g}{A_1ba^2}, \frac{F_{11}g}{A_1b^2h}, \frac{F_{12}g}{A_1ba^2}, \frac{C_{66}g}{A_1ba}, -2 \frac{E_{66}g}{A_1ba^2}, 2 \frac{F_{66}g}{A_1ba^2} \right),$$

$$\vartheta_{68.85} = \left(\frac{I_0}{A_1} \right)^{-0.5} \left(\frac{F_{66}g}{A_1a^2h}, \frac{C_{11}hg}{A_1b^3}, \frac{F_{66}g}{A_1bah} \right), \frac{C_{11}h^2}{A_1b^3}, \frac{A_4h^2}{A_1b^3}, \frac{3}{4} \frac{P_4h}{A_1ba^2}, -\frac{E_{12}h}{A_1ba^2}, -2 \frac{E_{66}h}{A_1ba^2}, -\frac{1}{8} \frac{P_2h}{A_1b^2a^2},$$

$$\quad (B22)$$

$$\frac{1}{8} \frac{P_2h}{A_1b^3a}, \frac{1}{8} \frac{P_2h}{A_1b^3a}, \frac{F_{12}h}{A_1ba^2}, 2 \frac{F_{66}h}{A_1ba^2}, \frac{3}{8} \frac{P_9h}{A_1ba^2}, -\frac{C^2I_5h}{A_1b^3}, \frac{C^2I_4h}{A_1b^3}, \left(\frac{I_0}{A_1} \right)^{-0.5} \left(\frac{C_{11}g}{A_1b^2}, -\frac{E_{11}g}{A_1b^3} \right).$$

$$\varpi_{1.7} = \frac{h^2}{b^2}, \frac{h^2}{a^2}, -\frac{I_1}{I_0a}, \frac{I_3}{I_0a}, \frac{I_2}{I_0a^2}, -2 \frac{I_4}{I_0a^2}, \frac{I_5}{I_0a^2},$$

$$\quad (B23)$$

$$\varpi_{8.20} = \frac{I_2}{I_0b^2}, -2 \frac{I_4}{I_0b^2}, \frac{I_5}{I_0b^2}, -\frac{I_1}{I_0b}, \frac{I_3}{I_0b}, \frac{h^3H1^2\eta}{A_1a^2}, -\frac{h^3H2^2\eta}{A_1a^2}, -\frac{h^2C^2I_0}{A_1a^2}, 2 \frac{h^2Ve_{31}}{A_1a^2}, 2 \frac{h^2Ve_{31f}}{A_1a^2}, \frac{1}{2} \frac{h^4A_1}{A_1b^4}, -\frac{h^3A_4}{A_1b^4}, \frac{h^3B_{11}}{A_1b^4},$$

$$\quad (B24)$$

$$\varpi_{21.32} = \frac{h^3A_2}{A_1a^4}, \frac{h^3A_4}{A_1a^4}, \frac{h^3B_{11}}{A_1a^4}, -2 \frac{h^2D_{12}}{A_1a^2b^2}, -4 \frac{h^2D_{66}}{A_1a^2b^2}, 2 \frac{h^2E_{12}}{A_1a^2b^2}, -\frac{h^2P_1}{A_1a^2b^2}, \frac{1}{2} \frac{h^2P_4}{A_1a^2b^2}, \frac{h^2B_{12}}{A_1a^2b}, 2 \frac{h^2B_{66}}{A_1a^2b}, \frac{h^2B_{12}}{A_1ab^2}, 2 \frac{h^2B_{66}}{A_1ab^2},$$

$$\quad (B25)$$

$$\varpi_{33.43} = \frac{h^3A_2}{A_1b^4}, -2 \frac{h^2C^3I_1}{A_1b^3}, 2 \frac{h^2C^3I_3}{A_1b^3}, -\frac{C^2I_4h}{A_1b^3}, \frac{C^2I_5h}{A_1b^3}, \frac{C^2I_4h}{A_1a^3}, \frac{C^2I_5h}{A_1a^3}, \frac{E_{12}h}{A_1ba^2}, 2 \frac{E_{66}h}{A_1ba^2}, \frac{1}{4} \frac{hP_{24}}{A_1ba^2}, \frac{E_{12}h}{A_1ab^2},$$

$$\quad (B26)$$

$$\begin{aligned} \varpi_{44..67} = & 2 \frac{E_{66} h}{A_{11} a b^2} \cdot \frac{1}{4} \frac{h P_{24}}{A_{11} a b^2} \cdot \left(\frac{I_0}{A_{11}} \right)^{-0.5} \left(\frac{E_{11} g}{A_{11} b^3}, \frac{E_{11} g}{A_{11} a^3}, -2 \frac{C I_4}{A_{11} b^2}, 2 \frac{C I_5}{A_{11} b^2}, -2 \frac{C I_4}{A_{11} a^2}, 2 \frac{C I_5}{A_{11} a^2} \right) \cdot -2 \frac{h^2 C^3 I_1}{A_{11} a^3}, \\ & 2 \frac{h^2 C^3 I_3}{A_{11} a^3}, \frac{h^2 C^2 I_2}{A_{11} b^4}, -2 \frac{h^2 C^2 I_4}{A_{11} b^4}, \frac{h^2 C^2 I_5}{A_{11} b^4}, \frac{h^2 C^2 I_2}{A_{11} a^4}, -2 \frac{h^2 C^2 I_4}{A_{11} a^4}, \frac{h^2 C^2 I_5}{A_{11} a^4}, \frac{h^2 A_4}{A_{11} b^3}, \frac{h^3 A_1}{A_{11} b^3}, -\frac{h^3 H 1^2 \eta}{A_{11} b^2}, \frac{h^3 H 2^2 \eta}{A_{11} b^2}, \\ & 2 \frac{h^2 V e_{31}}{A_{11} a^2}, 2 \frac{h^2 V e_{31 f}}{A_{11} a^2}, 2 \frac{h^3 B_{12}}{A_{11} a^2 b^2}, 2 \frac{h^3 B_{66}}{A_{11} a^2 b^2}, \end{aligned} \tag{B27}$$

$$\begin{aligned} \varpi_{68..90} = & \frac{1}{2} \frac{h^4 A_1}{A_{11} a^4}, \frac{h^2 A_4}{A_{11} a^3}, \frac{h^3 A_1}{A_{11} a^3}, -\frac{I_4}{h I_0 b}, \frac{I_5}{h I_0 b}, -\frac{I_4}{h I_0 a}, \frac{I_5}{h I_0 a}, -\frac{h^2 A_3}{A_{11} b^4}, 2 \frac{h^2 A_5}{A_{11} b^4}, -\frac{h^2 A_6}{A_{11} b^4}, \frac{h^2 D_{11}}{A_{11} b^4}, \frac{h^2 E_{11}}{A_{11} b^4}, \\ & -\frac{1}{2} \frac{h^2 P_1}{A_{11} b^4}, \frac{1}{4} \frac{h^2 P_4}{A_{11} b^4}, -\frac{h^2 A_3}{A_{11} a^4}, 2 \frac{h^2 A_5}{A_{11} a^4}, -\frac{h^2 A_6}{A_{11} a^4}, \frac{h A_5}{A_{11} b^3}, -\frac{h A_6}{A_{11} b^3}, \frac{h E_{11}}{A_{11} b^3}, \frac{1}{4} \frac{h P_4}{A_{11} b^3}, \frac{h A_5}{A_{11} a^3}, -\frac{h A_6}{A_{11} a^3}, \end{aligned} \tag{B28}$$

$$\begin{aligned} \varpi_{91..111} = & \frac{h E_{11}}{A_{11} a^3}, \frac{1}{4} \frac{h P_{24}}{A_{11} a^2}, \frac{h^2 B_1}{A_{11} a^2}, \frac{h^2 B_2}{A_{11} a^2}, \frac{h^2 B_1}{A_{11} b^2}, \frac{h^2 B_2}{A_{11} b^2}, \frac{h^2 B_{11}}{A_{11} a^3}, \frac{h^2 A_2}{A_{11} a^3}, -\frac{h^2 A_4}{A_{11} a^3}, \frac{h^3 B_{11}}{A_{11} b^4}, \frac{h^3 B_{11}}{A_{11} a^4}, \\ & -\frac{h^4 k_{winter}}{A_{11}}, \frac{h^2 D_{11}}{A_{11} a^4}, \frac{h^2 E_{11}}{A_{11} a^4}, -\frac{1}{2} \frac{h^2 P_1}{A_{11} a^4}, \frac{1}{4} \frac{h^2 P_4}{A_{11} a^4}, \frac{h^2 B_{11}}{A_{11} b^3}, \frac{h^2 A_2}{A_{11} b^3}, -\frac{h^2 A_4}{A_{11} b^3}, -2 \frac{h^3 e_{32} e_{15}}{\pi A_{11} b^2 \xi_{11} a}, -1, \end{aligned} \tag{B29}$$

$$\begin{aligned} \varpi_{112..132} = & \left(\frac{I_0}{A_{11}} \right)^{-0.5} \left(-\frac{h c_d}{A_{11}}, \frac{g E_{12}}{A_{11} a^2 b}, 2 \frac{g E_{66}}{A_{11} a b^2}, \frac{h g E_{11}}{A_{11} b^4}, -\frac{h g D_{11}}{A_{11} b^4}, -\frac{h g D_{11}}{A_{11} a^4}, 2 \frac{g E_{66}}{A_{11} a^2 b}, \frac{g E_{12}}{A_{11} a b^2}, \frac{h B_{11} g}{A_{11} a^3} \right) \cdot 2 \frac{h^3 B_{66}}{A_{11} a^2 b^2}, \\ & -\frac{h^3 Q_{11} T \alpha_{11}}{A_{11} a^2}, -\frac{h^3 Q_{12} T \alpha_{22}}{A_{11} a^2}, -\frac{h^3 Q_{13} T \alpha_{11}}{A_{11} a^2}, -\frac{h^3 Q_{12} T \alpha_{22}}{A_{11} a^2}, -\frac{h^3 Q_{12} T \alpha_{11}}{A_{11} b^2}, -\frac{h^3 Q_{22} T \alpha_{22}}{A_{11} b^2}, -\frac{h^3 Q_{123} T \alpha_{11}}{A_{11} b^2}, \\ & -\frac{h^3 Q_{22} T \alpha_{22}}{A_{11} b^2}, \frac{h^3 B_{12}}{A_{11} a^2 b^2}, 2 \frac{h^3 B_{66}}{A_{11} a^2 b^2}, \frac{h^3 B_{12}}{A_{11} a^2 b^2}, \end{aligned} \tag{B30}$$

$$\begin{aligned} \varpi_{133..150} = & 2 \frac{h^3 B_{66}}{A_{11} a^2 b^2}, 4 \frac{h^3 H 1 H 2 \eta}{A_{11} a b}, \frac{h^2 e_{32} B_{77} e_{15}}{A_{11} \xi_{11} b^2}, \left(\frac{I_0}{A_{11}} \right)^{-0.5} \left(2 \frac{h^2 g B_{11}}{A_{11} b^4}, \frac{h^2 g B_{11}}{A_{11} b^4}, \frac{h^2 g B_{11}}{A_{11} a^4}, \frac{h^2 e_{31} B_{77} e_{15}}{A_{11} \xi_{11} a^2} \right), \\ & \left(\frac{I_0}{A_{11}} \right)^{-0.5} \left(2 \frac{h^2 g B_{11}}{A_{11} a^4}, \frac{h^2 g B_{11}}{A_{11} b^4}, \frac{h^2 g B_{11}}{A_{11} a^4}, \frac{h g B_{12}}{A_{11} a b^2}, 2 \frac{h g B_{66}}{A_{11} a^2 b}, \frac{h g B_{12}}{A_{11} a^2 b}, 2 \frac{h g B_{66}}{A_{11} a^2 b} \right), \\ & \left(-2 \frac{h g D_{12}}{A_{11} a^2 b^2}, -4 \frac{h g E_{66}}{A_{11} a^2 b^2}, 2 \frac{h g E_{12}}{A_{11} a^2 b^2}, 4 \frac{h g E_{66}}{A_{11} a^2 b^2} \right), \end{aligned} \tag{B31}$$

$$\begin{aligned} \varpi_{151..176} = & -2 \frac{h^4 e_{31} e_{15}}{\pi A_{11} a^3 \xi_{11}}, \left(\frac{I_0}{A_{11}} \right)^{-0.5} \left(2 \frac{h^2 g B_{66}}{A_{11} a^2 b^2}, \frac{h^2 g B_{12}}{A_{11} a^2 b^2}, 2 \frac{h^2 g B_{66}}{A_{11} a^2 b^2}, \frac{h^2 g B_{12}}{A_{11} a^2 b^2}, 2 \frac{h^2 g B_{66}}{A_{11} a^2 b^2}, 4 \frac{h^2 g B_{12}}{A_{11} a^2 b^2}, 4 \frac{h^2 g B_{66}}{A_{11} a^2 b^2}, \frac{h^2 g B_{12}}{A_{11} a^2 b^2} \right) \\ & \left(2 \frac{h^2 g B_{66}}{A_{11} a^2 b^2}, \frac{h^2 g B_{12}}{A_{11} a^2 b^2}, 2 \frac{h^2 g B_{66}}{A_{11} a^2 b^2}, 2 \frac{h^2 g B_{66}}{A_{11} a^2 b^2}, 2 \frac{h C I_2}{A_{11} b^3}, \frac{h g E_{11}}{A_{11} a^4}, -2 \frac{h I_0 C}{A_{11} a}, -4 \frac{h C I_4}{A_{11} b^3} \right) \\ & \left(2 \frac{h C I_5}{A_{11} b^3}, -4 \frac{h C I_4}{A_{11} a^3}, 2 \frac{h C I_5}{A_{11} a^3}, -2 \frac{h C I_1}{A_{11} b^2}, 2 \frac{h C I_3}{A_{11} b^2}, -2 \frac{h C I_1}{A_{11} a^2}, 2 \frac{h C I_3}{A_{11} a^2}, \frac{h B_{11} g}{A_{11} b^3}, 2 \frac{h C I_2}{A_{11} a^3} \right) \end{aligned} \tag{B32}$$

$$\eta_{1..13} = \frac{R_1 h}{a^2}, \frac{R_1}{a}, \frac{1}{2} \frac{h}{a}, \frac{e_{24} R_1 h}{e_{15} b^2}, \frac{e_{24} R_1}{e_{15} b}, \frac{1}{2} \frac{\xi_{22} h a}{\xi_{11} b^2}, \frac{2 e_{31} h^2}{e_{15} a^2 \pi}, \frac{e_{31} R_5 h}{e_{15} a^2}, \frac{e_{31} R_5}{e_{15} a}, \frac{2 e_{32} h^2}{e_{15} b^2 \pi}, \frac{e_{32} R_5 h}{e_{15} b^2}, \frac{e_{32} R_5}{e_{15} b}, \frac{1}{2} \frac{\xi_{33} a \pi^2}{\xi_{11} h}. \tag{B33}$$

$$R_{1..6} = \int_{-h/2}^{h/2} \left(f(z) \cdot \cos\left(\frac{\pi z}{h}\right), \left(\cos\left(\frac{\pi z}{h}\right)\right)^2, \frac{\pi}{h} \sin\left(\frac{\pi z}{h}\right), z \frac{\pi}{h} \sin\left(\frac{\pi z}{h}\right), f(z) \frac{\pi}{h} \sin\left(\frac{\pi z}{h}\right), \left(\frac{\pi}{h} \sin\left(\frac{\pi z}{h}\right)\right)^2 \right) dz. \tag{B34}$$

$$P_{1..10} = \int_{-h/2}^{h/2} 2 G I_2^2 \left(1, f(z), f^2(z), f(z)_{,z}, f(z)_{,zz}, f(z) f(z)_{,z}, f(z) f(z)_{,zz} \right) dz, P_{11..14} = \int_{-h/2}^{h/2} \left(1, z, f(z), f(z)_{,z} \right) dz. \tag{B35}$$

References

- [1] L. E. Foster, 2005, *Nanotechnology: science, innovation, and opportunity*, Prentice Hall PTR,
- [2] G. L. Hornyak, J. J. Moore, H. F. Tibbals, J. Dutta, 2018, *Fundamentals of nanotechnology*, CRC press,
- [3] G. E. Mase, G. Mase, 1970, *Continuum mechanics*, McGraw-Hill New York,
- [4] J. N. Reddy, 2013, *An introduction to continuum mechanics*, Cambridge university press,
- [5] V. Bolotin, *The Dynamic Stability of Elastic Systems*, 1964.
- [6] A. H. Nayfeh, D. T. Mook, 2008, *Nonlinear oscillations*, John Wiley & Sons,
- [7] D. Gay, 2022, *Composite materials: design and applications*, CRC press,
- [8] J. R. Vinson, T.-W. Chou, *Composite materials and their use in structures*, 1975.
- [9] W. G. Cady, 2018, *Piezoelectricity: Volume Two: An Introduction to the Theory and Applications of Electromechanical Phenomena in Crystals*, Courier Dover Publications,
- [10] C. Lu, A. W. Czanderna, 2012, *Applications of piezoelectric quartz crystal microbalances*, Elsevier,
- [11] A. G. Arani, E. Haghparast, H. Zarei, Vibration analysis of functionally graded nanocomposite plate moving in two directions, *Steel and Composite Structures*, Vol. 23, No. 5, pp. 529-41, 2017.
- [12] K. Bouafia, M. M. Selim, F. Bourada, A. A. Bousahla, M. Bourada, A. Tounsi, E. Adda Bedia, A. Tounsi, Bending and free vibration characteristics of various compositions of FG plates on elastic foundation via quasi 3D HSDT model, *Steel and Composite Structures*, Vol. 41, No. 4, pp. 487-503, 2021.
- [13] M. Guellil, H. Saidi, F. Bourada, A. A. Bousahla, A. Tounsi, M. M. Al-Zahrani, M. Hussain, S. Mahmoud, Influences of porosity distributions and boundary conditions on mechanical bending response of functionally graded plates resting on Pasternak foundation, *Steel and Composite Structures*, Vol. 38, No. 1, pp. 1-15, 2021.
- [14] R. S. Chahar, B. Kumar, Effectiveness of piezoelectric fiber reinforced composite laminate in active damping for smart structures, *Steel and Composite Structures*, Vol. 31, No. 4, pp. 387-396, 2019.
- [15] N. Djilali, A. A. Bousahla, A. Kaci, M. M. Selim, F. Bourada, A. Tounsi, A. Tounsi, K. H. Benrahou, S. Mahmoud, Large cylindrical deflection analysis of FG carbon nanotube-reinforced plates in thermal environment using a simple integral HSDT, *Steel and Composite Structures*, Vol. 42, No. 6, pp. 779-789, 2022.
- [16] F. Abad, J. Rouzegar, S. Lotfian, Application of the exact spectral element method in the analysis of the smart functionally graded plate, *Steel and Composite Structures*, Vol. 47, No. 2, pp. 297-313, 2023.
- [17] K. Draiche, M. M. Selim, A. A. Bousahla, A. Tounsi, F. Bourada, A. Tounsi, S. Mahmoud, A computational investigation on flexural response of laminated composite plates using a simple quasi-3D HSDT, *Steel and Composite Structures*, Vol. 41, No. 5, pp. 697-711, 2021.
- [18] A. Ameri, A. Fekrar, F. Bourada, M. M. Selim, K. H. Benrahou, A. Tounsi, M. Hussain, Hygro-thermo-mechanical bending of laminated composite plates using an innovative computational four variable refined quasi-3D HSDT model, *Steel and Composite Structures*, Vol. 41, No. 1, pp. 31-44, 2021.
- [19] Q.-H. Pham, P.-C. Nguyen, V.-K. Tran, T. Nguyen-Thoi, Finite element analysis for functionally graded porous nano-plates resting on elastic foundation, *Steel and Composite Structures*, Vol. 41, No. 2, pp. 149-166, 2021.
- [20] A. Attia, A. T. Berrabah, A. A. Bousahla, F. Bourada, A. Tounsi, S. Mahmoud, Free vibration analysis of FG plates under thermal environment via a simple 4-unknown HSDT, *Steel and Composite Structures*, Vol. 41, No. 6, pp. 899-910, 2021.
- [21] Z. Wang, Y. Chen, Assessment of multi-physical field effects on nonlinear static stability behavior of nanoshells based on a numerical approach, *Steel and Composite Structures*, Vol. 46, No. 4, pp. 513, 2023.
- [22] M. A. Alazwari, A. A. Abdelrahman, A. Wagih, M. A. Eltaher, H. E. Abd-El-Mottaleb, Static analysis of cutout microstructures incorporating the microstructure and surface effects, *Steel and Composite Structures*, Vol. 38, No. 5, pp. 583-597, 2021.
- [23] F. Z. Kettaf, M. Beguediab, S. Benguediab, M. M. Selim, A. Tounsi, M. Hussain, Mechanical and thermal buckling analysis of laminated composite plates, *Steel and Composite Structures*, Vol. 40, No. 5, pp. 697-708, 2021.
- [24] F. Zhang, Z. Cao, Y. Qiao, D. Liu, G. Yao, Parametric Vibration Stability Analysis of an Axially Moving Plate with Periodical Distributed Materials, *Journal of Vibration Engineering & Technologies*, pp. 1-11, 2023.
- [25] T. Cao, Y. Hu, Magnetoelastic primary resonance and bifurcation of an axially moving ferromagnetic plate under harmonic magnetic force, *Communications in Nonlinear Science and Numerical Simulation*, Vol. 117, pp. 106974, 2023.

- [26] F. L. Yang, Y. Q. Wang, Y. Liu, Low-velocity impact response of axially moving functionally graded graphene platelet reinforced metal foam plates, *Aerospace Science and Technology*, Vol. 123, pp. 107496, 2022.
- [27] A. G. Arani, M. E. Shahraki, E. Haghparast, Instability analysis of axially moving sandwich plates with a magnetorheological elastomer core and GNP-reinforced face sheets, *Journal of the Brazilian Society of Mechanical Sciences and Engineering*, Vol. 44, No. 4, pp. 150, 2022.
- [28] Y. Wang, H. Wu, F. Yang, Q. Wang, An efficient method for vibration and stability analysis of rectangular plates axially moving in fluid, *Applied Mathematics and Mechanics*, Vol. 42, No. 2, pp. 291-308, 2021.
- [29] Y.-F. Zhou, Z.-M. Wang, Dynamic instability of axially moving viscoelastic plate, *European Journal of Mechanics-A/Solids*, Vol. 73, pp. 1-10, 2019.
- [30] A. G. Arani, T. Soleymani, Size-dependent vibration analysis of an axially moving sandwich beam with MR core and axially FGM faces layers in yawed supersonic airflow, *European Journal of Mechanics-A/Solids*, Vol. 77, pp. 103792, 2019.
- [31] P. Hung, P. Phung-Van, C. H. Thai, Small scale thermal analysis of piezoelectric–piezomagnetic FG microplates using modified strain gradient theory, *International Journal of Mechanics and Materials in Design*, pp. 1-23, 2023.
- [32] M. Arefi, E. M.-R. Bidgoli, T. Rabczuk, Thermo-mechanical buckling behavior of FG GNP reinforced micro plate based on MSGT, *Thin-Walled Structures*, Vol. 142, pp. 444-459, 2019.
- [33] A. Ghorbanpour Arani, B. Rousta Navi, M. Mohammadimehr, S. Niknejad, A. Ghorbanpour Arani, A. Hosseinpour, Pull-in instability of MSGT piezoelectric polymeric FG-SWCNTs reinforced nanocomposite considering surface stress effect, *Journal of Solid Mechanics*, Vol. 11, No. 4, pp. 759-777, 2019.
- [34] P. Kumar, S. Harsha, Static, buckling and vibration response analysis of three-layered functionally graded piezoelectric plate under thermo-electric mechanical environment, *Journal of Vibration Engineering & Technologies*, Vol. 10, No. 4, pp. 1561-1598, 2022.
- [35] A. Singh, S. Naskar, P. Kumari, T. Mukhopadhyay, Viscoelastic free vibration analysis of in-plane functionally graded orthotropic plates integrated with piezoelectric sensors: Time-dependent 3D analytical solutions, *Mechanical Systems and Signal Processing*, Vol. 184, pp. 109636, 2023.
- [36] Y. Zhao, X. Hou, S. Zhang, T. Sun, L. Du, Z. Deng, Nonlinear forced vibration of thermo-electro-elastic piezoelectric-graphene composite nanoplate based on viscoelastic foundation, *Acta Mechanica Sinica*, Vol. 39, No. 3, pp. 522228, 2023.
- [37] A. Sofiyev, On the Solution of Dynamic Stability Problem of Functionally Graded Viscoelastic Plates with Different Initial Conditions in Viscoelastic Media, *Mathematics*, Vol. 11, No. 4, pp. 823, 2023.
- [38] Z. Li, J. Liu, B. Hu, Y. Wang, H. Shen, Wave propagation analysis of porous functionally graded piezoelectric nanoplates with a visco-Pasternak foundation, *Applied Mathematics and Mechanics*, Vol. 44, No. 1, pp. 35-52, 2023.
- [39] P. H. Cong, N. D. Duc, Effect of nonlocal parameters and Kerr foundation on nonlinear static and dynamic stability of micro/nano plate with graphene platelet reinforcement, *Thin-Walled Structures*, Vol. 182, pp. 110146, 2023.
- [40] M. H. Jalaei, H.-T. Thai, Dynamic stability of viscoelastic porous FG nanoplate under longitudinal magnetic field via a nonlocal strain gradient quasi-3D theory, *Composites Part B: Engineering*, Vol. 175, pp. 107164, 2019.
- [41] Q.-H. Pham, P.-C. Nguyen, Dynamic stability analysis of porous functionally graded microplates using a refined isogeometric approach, *Composite Structures*, Vol. 284, pp. 115086, 2022.
- [42] J. Shi, X. Teng, Modified size-dependent theory for investigation of dynamic stability and critical voltage of piezoelectric curved system, *Composite Structures*, Vol. 301, pp. 116210, 2022.
- [43] Q. Li, D. Wu, W. Gao, D. Hui, Nonlinear dynamic stability analysis of axial impact loaded structures via the nonlocal strain gradient theory, *Applied Mathematical Modelling*, Vol. 115, pp. 259-278, 2023.
- [44] Y. Zhang, L. Ma, W. Zhang, X. Gu, Nonlinear dynamic responses of functionally graded graphene platelet reinforced composite cantilever rotating warping plate, *Applied Mathematical Modelling*, Vol. 113, pp. 44-70, 2023.
- [45] A. A. Daikh, M. S. A. Houari, M. O. Belarbi, S. A. Mohamed, M. A. Eltaher, Static and dynamic stability responses of multilayer functionally graded carbon nanotubes reinforced composite nanoplates via quasi 3D nonlocal strain gradient theory, *Defence Technology*, Vol. 18, No. 10, pp. 1778-1809, 2022.
- [46] S. Lu, N. Xue, W. Zhang, X. Song, W. Ma, Dynamic stability of axially moving graphene reinforced laminated composite plate under constant and varied velocities, *Thin-Walled Structures*, Vol. 167, pp. 108176, 2021.

- [47] X. Guo, S. Wang, L. Sun, D. Cao, Dynamic responses of a piezoelectric cantilever plate under high–low excitations, *Acta Mechanica Sinica*, Vol. 36, pp. 234-244, 2020.
- [48] R. Abdikarimov, M. Amabili, N. I. Vatin, D. Khodzhaev, Dynamic stability of orthotropic viscoelastic rectangular plate of an arbitrarily varying thickness, *Applied Sciences*, Vol. 11, No. 13, pp. 6029, 2021.
- [49] A. Shariati, S. H. S. Hosseini, F. Ebrahimi, A. Toghroli, Nonlinear dynamics and vibration of reinforced piezoelectric scale-dependent plates as a class of nonlinear Mathieu–Hill systems: parametric excitation analysis, *Engineering with Computers*, Vol. 37, pp. 2285-2301, 2021.
- [50] J.-X. Wang, W.-Q. Wang, S. Gao, A novel composite joint with corrugated web and cover plates for simultaneously improving anti-collapse resistance and seismic behavior, *Archives of Civil and Mechanical Engineering*, Vol. 23, No. 2, pp. 77, 2023.
- [51] C. Chu, M. Al-Furjan, R. Kolahchi, Energy harvesting and dynamic response of SMA nano conical panels with nanocomposite piezoelectric patch under moving load, *Engineering Structures*, Vol. 292, pp. 116538, 2023.
- [52] P. Wan, M. Al-Furjan, R. Kolahchi, L. Shan, Application of DQHFEM for free and forced vibration, energy absorption, and post-buckling analysis of a hybrid nanocomposite viscoelastic rhombic plate assuming CNTs' waviness and agglomeration, *Mechanical Systems and Signal Processing*, Vol. 189, pp. 110064, 2023.
- [53] J. Lou, L. He, J. Du, A unified higher order plate theory for functionally graded microplates based on the modified couple stress theory, *Composite Structures*, Vol. 133, pp. 1036-1047, 2015.
- [54] J. N. Reddy, 2003, *Mechanics of laminated composite plates and shells: theory and analysis*, CRC press,
- [55] R. Kolahchi, A. Cheraghbak, Agglomeration effects on the dynamic buckling of viscoelastic microplates reinforced with SWCNTs using Bolotin method, *Nonlinear Dynamics*, Vol. 90, No. 1, pp. 479-492, 2017.
- [56] M. Mohammadimehr, N. B. ROUSTA, A. A. Ghorbanpour, Eshelby-mori-tanaka and the extended mixture rule approaches for nonlocal vibration of piezoelectric nanocomposite plate with considering surface stress and magnetic field effects, 2014.
- [57] R. Ansari, S. Sahmani, Surface stress effects on the free vibration behavior of nanoplates, *International Journal of Engineering Science*, Vol. 49, No. 11, pp. 1204-1215, 2011.
- [58] T. Mori, K. Tanaka, Average stress in matrix and average elastic energy of materials with misfitting inclusions, *Acta metallurgica*, Vol. 21, No. 5, pp. 571-574, 1973.
- [59] M. Arefi, M. Kiani, Magneto-electro-mechanical bending analysis of three-layered exponentially graded microplate with piezomagnetic face-sheets resting on Pasternak's foundation via MCST, *Mechanics of Advanced Materials and Structures*, Vol. 27, No. 5, pp. 383-395, 2020.
- [60] C. Ru, Simple geometrical explanation of Gurtin-Murdoch model of surface elasticity with clarification of its related versions, *Science China Physics, Mechanics and Astronomy*, Vol. 53, No. 3, pp. 536-544, 2010.
- [61] R. Kolahchi, H. Hosseini, M. Esmailpour, Differential cubature and quadrature-Bolotin methods for dynamic stability of embedded piezoelectric nanoplates based on visco-nonlocal-piezoelectricity theories, *Composite Structures*, Vol. 157, pp. 174-186, 2016.
- [62] A. G. Arani, R. Kolahchi, M. S. Zarei, Visco-surface-nonlocal piezoelectricity effects on nonlinear dynamic stability of graphene sheets integrated with ZnO sensors and actuators using refined zigzag theory, *Composite Structures*, Vol. 132, pp. 506-526, 2015.
- [63] A. Ghorbanpour Arani, M. Maboudi, A. Ghorbanpour Arani, S. Amir, 2D-magnetic field and biaxial in-plane pre-load effects on the vibration of double bonded orthotropic graphene sheets, *Journal of Solid Mechanics*, Vol. 5, No. 2, pp. 193-205, 2013.
- [64] T. Murmu, M. McCarthy, S. Adhikari, In-plane magnetic field affected transverse vibration of embedded single-layer graphene sheets using equivalent nonlocal elasticity approach, *Composite Structures*, Vol. 96, pp. 57-63, 2013.
- [65] A. G. Arani, E. Haghparast, H. B. A. Zarei, Vibration of axially moving 3-phase CNTFPC plate resting on orthotropic foundation, *Structural Engineering and Mechanics*, Vol. 57, No. 1, pp. 105-126, 2016.
- [66] P. Sourani, M. Hashemian, M. Pirmoradian, D. Toghraie, A comparison of the Bolotin and incremental harmonic balance methods in the dynamic stability analysis of an Euler–Bernoulli nanobeam based on the nonlocal strain gradient theory and surface effects, *Mechanics of Materials*, Vol. 145, pp. 103403, 2020.
- [67] M. Hashemian, M. Falsafioon, M. Pirmoradian, D. Toghraie, Nonlocal dynamic stability analysis of a Timoshenko nanobeam subjected to a sequence of moving nanoparticles considering surface effects, *Mechanics of Materials*, Vol. 148, pp. 103452, 2020.